Ecological Engineering 148 (2020) 105786

Contents lists available at ScienceDirect

Ecological Engineering

journal homepage: www.elsevier.com/locate/ecoleng

Nitrate removal and secondary effects of a woodchip bioreactor for the treatment of subsurface drainage with dynamic flows under pastoral agriculture

Aldrin Rivas[a,*], Greg Barkle[b], Roland Stenger[a], Brian Moorhead[a], Juliet Clague[a]

[a] Lincoln Agritech Ltd., Private Bag 3062, Hamilton 3240, New Zealand
[b] Land and Water Research Ltd., PO Box 27046, Garnett Ave., Hamilton 3257, New Zealand

ARTICLE INFO

Keywords:
Denitrification
Artificial drainage
Greenhouse gas
Reactive filter
Pollution swapping
Dissolved reactive phosphorus

ABSTRACT

While enabling economically viable use of poorly drained soils, artificial subsurface drainage has also been found to be a significant pathway for nutrient transfers from agricultural land to surface waters. Thus, mitigating the impacts of agriculture on surface water quality needs to address nutrient transfers via subsurface drainage. Woodchip bioreactors are a promising mitigation option as demonstrated under arable agriculture in the mid-west of the USA. However, research is needed to ascertain their efficiency in removing nutrients from very flashy drainage flows common in New Zealand (NZ) pastoral agriculture and any possible pollution swapping (e.g. reduction of leaching losses vs. greenhouse gas emissions). Accordingly, a lined 78-m^3 woodchip bioreactor was constructed on a dairy farm in the Hauraki Plains (Waikato, NZ) with a drainage area of 0.65 ha. Rainfall, flow, hydrochemistry and dissolved gases in the inflow and outflow were monitored for two drainage seasons (part of 2017, 2018). Based on the nitrate-N fluxes, the estimated nitrate removal efficiency of the bioreactor was 99 and 48% in 2017 and 2018, respectively. The higher removal efficiency in 2017 could be attributed to two reasons. Firstly, the substantially longer hydraulic residence time (HRT) of the water in the bioreactor (mean = 21.1 days vs 4.7 days in 2018) provided more opportunity for microorganisms to reduce the nitrate. A strong positive relationship between HRT and removal efficiency was also observed within the 2018 drainage season. Secondly, denitrification was supported in 2017 by greater electron donor availability. Evidence of this was the higher mass of DOC discharge from the bioreactor (318 mg C L^{-1} of bioreactor volume vs 165 mg C L^{-1} in 2018). Removal rates in the bioreactor varied from 0.67–1.60 g N m^{-3} day^{-1} and were positively correlated with inflow nitrate loads. Pollution swapping was observed during the start-up phase of the bioreactor in both years (DOC, and DRP only in 2017) and during periods with very long HRTs (hydrogen sulphide (H_2S) and methane (CH_4) production). Substantially elevated discharges of DOC and DRP, as compared to inlet conditions, occurred during the initial start-up phase of the bioreactor in 2017 (3 to 3.5 pore volumes of the bioreactor), but only slightly elevated DOC and decreased DRP discharges were observed when drainage flow resumed at the start of the 2018 drainage season. Unexpectedly, cumulative DRP removal during the 2018 drainage season amounted to 89% of the DRP inflow into the bioreactor. Long HRTs (> 5 days) enabled high nitrate removal efficiency (≥59%) and promoted complete reduction of nitrate to harmless dinitrogen gas but also promoted strongly reduced conditions, resulting in the production of H_2S and CH_4. On the other hand, short HRTs (< 4 days) only allowed for moderate nitrate removal efficiency (≤43%) and constrained complete reduction of nitrate resulting in higher nitrous oxide concentrations in the outflow as compared to the inflow. Thus, nitrate removals above 50% were not able to be achieved without inducing H_2S and CH_4 generation. However, it may be achievable when the microbial community is provided with an additional source of readily available carbon during the critical periods when hydraulic flow and concomitant N load peaks occur.

1. Introduction

Artificial drainage has been instrumental in the viable use of poorly drained soils for agriculture. However, artificial drains can also provide a pathway for the fast transfer of unattenuated nutrients to streams and rivers (Algoazany et al., 2007; King et al., 2015a; Arenas Amado et al.,

* Corresponding author at: Lincoln Agritech Ltd., Private Bag 3062, Hamilton, 3240, New Zealand.
E-mail address: aldrin.rivas@lincolnagritech.co.nz (A. Rivas).

https://doi.org/10.1016/j.ecoleng.2020.105786
Received 13 August 2019; Received in revised form 3 March 2020; Accepted 4 March 2020

2017). This is a concern as the contribution of tile drainage to streamflow has been found to range from 42 to 86% in catchment studies conducted in agricultural lands in Ohio and Illinois in the USA and in Ontario, Canada (King et al., 2015b). In an effort to mitigate the impacts of artificial drainage on surface water quality, several measures have been proposed, including controlled drainage (Tan et al., 1999; Ballantine and Tanner, 2013) and denitrifying bioreactors (Schipper et al., 2010; Christianson et al., 2012b; Addy et al., 2016). A denitrifying bioreactor is fundamentally a pit filled with a source of carbon (e.g. woodchips, corn husks), which microorganisms use to transform nitrate through the process of denitrification into gaseous forms of nitrogen, mostly dinitrogen gas (N_2). Denitrifying bioreactors have been used to treat shallow contaminated groundwater in the form of a permeable reactive barrier (sometimes referred to as 'denitrification wall') intercepting shallow lateral flow (Schipper and Vojvodic-Vukovic, 1998; Robertson et al., 2000; Schipper et al., 2005; Barkle et al., 2008). The technology has also been used to treat discharge from artificial drainage systems. This can occur at the edge of the field by intercepting tile drainage before it discharges into open drains or in the open drains themselves (as an in-ditch bioreactor) (Robertson and Merkley, 2009; Schipper et al., 2010; Addy et al., 2016; Pfannerstill et al., 2016; Christianson et al., 2017a; Sarris and Burbery, 2018). The earliest known field-scale application of a bioreactor for treating artificial drainage using woodchips was in the 1990s in Canada (Blowes et al., 1994; Robertson et al., 2000). Since then, the suitability of field-scale bioreactors as a mitigation option for the impacts of agricultural drainage has been investigated worldwide, such as in Canada (van Driel et al., 2006; Robertson et al., 2009; Husk et al., 2017), Denmark (Bruun et al., 2016b; Bruun et al., 2017; Carstensen et al., 2019), Germany (Pfannerstill et al., 2016), Ireland (Fenton et al., 2016), New Zealand (Hudson et al., 2018; Goeller et al., 2019), and the USA (Chun et al., 2010; Christianson et al., 2012a; Ghane et al., 2015; Hassanpour et al., 2017). In the US, bioreactors have already been accepted as one of the US Department of Agriculture's Conservation Practices (Standard No. 605) and are being adopted increasingly in cropped lands (Christianson et al., 2012a; Hartz et al., 2017). However, a different bioreactor design and operation than in the US is required for the shallower subsurface drainage systems in lowland areas with accompanying highly variable flows and nitrate concentrations common in many agricultural lands, including pastoral lands in New Zealand (NZ). These conditions contrast with the generally deeper drainage systems in the US, which are often fed by snow meltwater and therefore treat a much steadier inflow and N loadings (Hassanpour et al., 2017).

Several investigations on bioreactors have been conducted in NZ, but these were mainly under laboratory settings with controlled environments (Cameron and Schipper, 2010; Warneke et al., 2011c; Cameron and Schipper, 2012). Limited field-scale investigations dealt with treating wastewater effluents from domestic, glasshouse, dairy shed, or laboratories (Warneke et al., 2011a; Warneke et al., 2011b; Tanner et al., 2012; Rambags et al., 2016) or intercepting shallow groundwater as a 'denitrification wall' (Schipper et al., 2004; Schipper et al., 2005; Barkle et al., 2008; Long et al., 2011). Several field-scale studies targeted treating artificial drainage water (Hudson et al., 2018; Goeller et al., 2019), but these were either not on an area with highly variable and seasonal flows and/or not considering potential secondary effects.

Bioreactors have been found to be effective in removing nitrate from drainage water but detrimental side effects (i.e., pollution swapping) have also been reported. Removal efficiency (RE) of nitrate from artificial drainage by bioreactors has been reported to range from 12 to 76% of the nitrate load (Jaynes et al., 2008; Christianson et al., 2012b; Hassanpour et al., 2017). Removal rates (RR) have been found to vary between 0.01 and 15 g nitrate-N m^{-3} day^{-1} (Schipper et al., 2010; Christianson et al., 2012a; Addy et al., 2016; Hassanpour et al., 2017; Griessmeier et al., 2019). On the other hand, negative side effects include; high concentrations of dissolved organic matter and/or phosphorus in the outflow especially soon after installation, emission of greenhouse gases such as nitrous oxide (N_2O) and methane (CH_4), and production of odorous hydrogen sulphide gas (H_2S) (Schipper et al., 2010; Herbstritt, 2014; Healy et al., 2015; Weigelhofer and Hein, 2015). An incomplete denitrification process results in excess N_2O emitted through the surface of the bioreactor or discharged as dissolved gas in the outflow. Moreover, denitrification – being a microbially-mediated process – generally follows the succession of electron-accepting processes based on the energy generated (O_2 > NO_3^- > Mn (IV) > Fe (III) > SO_4^{2-} > CO_2) (McMahon and Chapelle, 2008). Thus, if the bioreactor has become strongly reduced with the absence or very low concentrations of dissolved oxygen (O_2) and nitrate, sulphate (SO_4^{2-}) and carbon dioxide (CO_2) reduction (methanogenesis) may occur, resulting in the production of H_2S and CH_4, respectively.

Several studies have looked into the relationships between environmental conditions (e.g. flow, temperature, etc.) and nitrate removal and/or greenhouse gas production, but these were mostly done in controlled settings in laboratories (Greenan et al., 2009; Christianson et al., 2011; Healy et al., 2012; Christianson et al., 2013a; Healy et al., 2015; Weigelhofer and Hein, 2015; Bruun et al., 2016a; Hoover et al., 2016; Lepine et al., 2016; Bock et al., 2018a; Soupir et al., 2018). There are also limited field-scale or in situ studies dealing with agricultural drainage water (Elgood et al., 2010; Christianson et al., 2013b; David et al., 2016; Hassanpour et al., 2017; Davis et al., 2019; Goeller et al., 2019; Martin et al., 2019). Moreover, some of these studies also applied constraints deviating from natural flow conditions (Davis et al., 2019; Martin et al., 2019). Thus the main objective of this research was to assess the applicability and performance of denitrifying bioreactor technology to reduce nitrate loads from subsurface drains with very flashy drainage flows and variable nitrate concentrations as common in New Zealand pastoral agriculture. We aimed to identify the factors affecting the performance and pollution-swapping side-effects of a bioreactor receiving highly variable pastoral drainage flows and concentrations, and to identify potential modifications to optimise its efficiency.

2. Methods

2.1. Study site

A pilot-scale denitrifying woodchip bioreactor (hereafter referred to as the Tatuanui bioreactor) was installed in March–July 2017 on a dairy farm in Tatuanui in the Waikato region of New Zealand. Artificial subsurface drainage is commonly installed in this lowland area to prevent shallow groundwater from rising seasonally into the root zone of the dairy pastures. The bioreactor intercepts drainage water from an artificial subsurface drain with a drainage area of approximately 0.65 ha. At the point of interception, the subsurface drain is located at approximately 0.7 m below ground surface.

The soil at the site was mapped as Typic Impeded Allophanic Soil (NZ Soil Classification) with a loamy texture throughout the soil zone (https://smap.landcareresearch.co.nz/). Sand dominates the profile from a depth of 1.05 m below ground surface (bgs), followed by a soft clayey layer of approximately 0.2 m thickness at a depth of about 1.80 m bgs.

2.2. Bioreactor design and operation

The Tatuanui bioreactor is trapezoidal in shape due to the sides being battered at 1:1 for safety reasons during construction, with a bottom footprint of 5 m × 9 m and a surface area of 8.4 m × 12.4 m (Fig. 1). The depth of the bioreactor floor is approximately 1.7 m bgs. The bioreactor was lined with ethylene propylene diene monomer (EPDM, 1.1 mm Firestone GeoGard) on the bottom and sides. The lined pit was filled with untreated Monterey pine (*Pinus radiata*) woodchips (median width = 8.6 mm and thickness = 0.8–13.1 mm; Fig. 2) to a

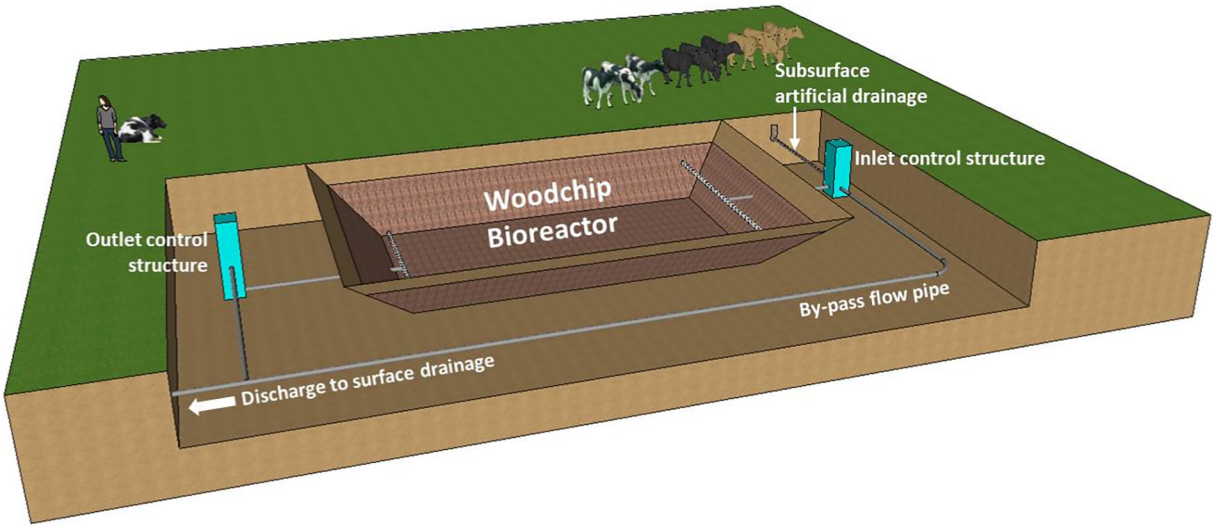

Fig. 1. Schematic showing the main components of the woodchip bioreactor installed in Tatuanui (Waikato, New Zealand).

Fig. 2. Untreated woodchips (*Pinus radiata*) used as source of electron donor in the Tatuanui bioreactor. Scale in the tape measure in mm.

height of 1.2 m from the bioreactor floor, resulting in a total bioreactor woodchip volume of approximately 78 m^3, about 20 m^3 of which was overburden to allow flexibility in operation if required and replenish the anticipated decrease in volume as woodchips age. Pine woodchips were chosen as the source of carbon as they are easily available in New Zealand and have been well studied (Cameron and Schipper, 2012; Burbery et al., 2014; Goeller et al., 2019). Geotextile membrane (Bidim A14, 155 g m^{-2}) was placed on top of the woodchips to avoid mixing woodchips with the soil backfill added on top. Control boxes made of polyvinyl chloride were installed at the inlet and outlet with V-notch weirs installed to measure flow. Bypass flow and flow through the bioreactor (i.e. outlet flow) were monitored every five minutes. Flow was computed from the head of water above the V-notch weir crotch in the control boxes monitored through a stilling well beside the control boxes equipped with pressure transducer (Fig. 3). Rain was monitored with a 0.2 mm tipping bucket rain gauge installed at the site and calibrated at the beginning of each season.

The bioreactor was sized to remove approximately 50% of the estimated annual nitrate-N loading. This was based on limited field information on nitrate concentrations and flow, and using a denitrification removal rate of 3.5 g N m^{-3} day^{-1} (Cameron and Schipper, 2012).

2.3. Sampling and analytical methods

2.3.1. Water and dissolved gas sampling

Inflow and outflow water samples were collected automatically by ISCO samplers (Model 3700) every 10 m^3 of flow from the control

Fig. 3. The completed installation of the Tatuanui woodchip bioreactor showing the main components: (1) inlet control structure with auto sampler and stilling well, (2) outlet control structure with auto sampler and stilling well, (3) rain gauge, solar panel, and control panels for the instruments.

boxes. Samples of 500 mL were collected in 1 L polypropylene (PP) bottles containing 3.5 mL of 5700 ppm mercuric chloride ($HgCl_2$) for sample preservation. Each batch of bottles collected from the samplers was stored in a fridge at the laboratory and transported on ice for analysis at the National Institute of Water and Atmospheric Research (NIWA) Water Quality Laboratory in Hamilton, New Zealand.

Water samples were also collected manually about every two weeks from the inlet and outlet control boxes before the water flows over the weir in three sets: duplicates of 100 mL glass bottles with crimp lids and containing 0.7 mL of 5700 ppm $HgCl_2$ as preservative for dissolved gases; 50 mL polyethylene (PE) bottles field-filtered to 0.45 μm for metals; and 100 mL PE bottles for pH and electrical conductivity (EC) measurements. Dissolved oxygen (O_2) was measured at the same time with a YSI ProODO probe from a subsample collected from the control boxes (in 2017) or in situ with the probe lowered into the inlet and outlet control box and a longitudinal mid-distance well (in 2018). While the procedure we used for measuring DO in the second year may be considered superior to the procedure we used in the first year, both procedures served our purpose of determining whether reduced conditions were achieved within the bioreactor. The very low (< 1 mg L^{-1}) DO concentrations observed in the outlet in both years show that this was clearly the case.

2.3.2. Hydrochemical analyses

A flow injection analyser was used at the NIWA Water Quality Laboratory in Hamilton to measure dissolved reactive phosphorus (DRP), nitrite + nitrate (NO_2-N + NO_3-N), ammoniacal N (NH_4-N), and total nitrogen (TN) and phosphorus (TP) (both after persulphate digestion) following APHA 4500 (Rice et al., 2012). Sulphate (SO_4^{2-}) was measured by ion chromatography following APHA 4110 B at the Watercare Laboratory Services in Auckland. Dissolved organic carbon (DOC) was measured at the Eurofins ELS Ltd. laboratory in Lower Hutt following APHA 5310 (B, C), whereas total organic carbon (TOC) was measured by IR detection following APHA 5310 B. The limits of detection were: 0.001 mg L^{-1} for DRP, NO_2-N + NO_3-N, NH_4-N, and TP; 0.01 mg L^{-1} for TN; 0.5 mg L^{-1} for SO_4^{2-}; 0.1 mg L^{-1} for DOC; and 0.2 mg L^{-1} for TOC.

Selected elements (arsenic, cadmium, chromium, copper, iron, manganese, and lead) were analysed by inductively coupled plasma optical emission spectrometry (ICP-OES) following APHA 3120 at Lincoln University, Lincoln. The limits of detection were: 0.0015 mg L^{-1} (arsenic), 0.0003 (cadmium), 0.0004 (chromium), 0.0006 (copper), 0.0007 (iron), 0.0001 (manganese), 0.0033 (lead).

2.3.3. Dissolved gas analyses

Dissolved gases were extracted from the 100 mL water samples and analysed at Lincoln University by gas chromatograph (SRI 8610C). Dissolved nitrous oxide (N_2O) was measured by gas chromatograph with electron capture detector (GC-ECD) (Mosier and Mack, 1980), whereas dissolved methane (CH_4) was measured by gas chromatograph with flame ionization detector (GC-FID) (McWilliam and Dewar, 1958).

2.4. Calculations and statistical analysis

2.4.1. Porosity and hydraulic conductivity

The drainable porosity of the bioreactor was estimated in situ, during the draining of the bioreactor at the end of each of the two drainage seasons, by dividing the volume of water pumped out by the bioreactor volume drained; the latter deduced from the water level in the bioreactor monitored during pumping. The average drainable porosity was 46.2%, a value in the middle of drainable porosities (37–56%) estimated in other studies (Cameron and Schipper, 2010; Cameron and Schipper, 2012; Burbery et al., 2014; Feyereisen and Christianson, 2015; Ghane et al., 2016). Additionally, permeameter tests were carried out using 0.1 m^3 of the same woodchip material packed to a very similar configuration (drainable porosity = 48.6%). The measured hydraulic conductivity of the woodchips was 26,680 m day^{-1}, the total porosity was 85.6%, and the packing densities were 584.6 kg m^{-3} for fresh woodchips and 215.3 kg m^{-3} for oven-dried woodchips. While total porosity and packing density values were comparable with other studies (Christianson et al., 2010; Burbery et al., 2014; Feyereisen and Christianson, 2015; Goodwin et al., 2015), the estimated hydraulic conductivity was two and half to six times the value estimated in other studies (Christianson et al., 2010; Burbery et al., 2014; Feyereisen and Christianson, 2015). The difference between the hydraulic conductivity estimates was attributed to the orientation of the chips and water flow direction: in the aforementioned studies, water flow was apparently 90° to the way woodchips were packed, i.e. into the face of woodchip, whereas in our test, water flow was parallel to the way woodchips were packed. We consider the latter setup more relevant, as it reflects more closely the flow direction through our bioreactor, i.e. inlet header at the top with flow mainly horizontal and down towards exit through the footer at the base of the bioreactor.

2.4.2. Hydraulic residence time

The hydraulic residence time (HRT) of drainage water in the bioreactor was estimated as:

$$HRT = \frac{\varnothing V_s}{Q} \quad (1)$$

where ϕ is the drainable or effective porosity, V_s is the saturated volume of the bioreactor, and Q is the flow through the bioreactor. The use of effective porosity provides a more accurate estimate of HRT compared to using the total porosity (Ghane et al., 2019). The saturated volume of the bioreactor was determined as 56.3 m^3. The measured outlet flow was used to describe flow through the bioreactor, which is justified provided there is no leak observed in the bioreactor (Ghane et al., 2019; Goeller et al., 2019).

While tracer tests could potentially provide a superior estimate of HRT compared to using information on measured flow and porosity, other studies using tracer tests were explicitly designed to investigate in detail the internal hydraulics or hydrodynamics of a bioreactor (Chun et al., 2010; Christianson et al., 2013b; Ghane et al., 2019). However, in this field investigation, with no flow control, a tracer test was considered unnecessary for the scope of our study. Moreover, the use of the nominal HRT as applied in this study is the common approach used in many similar published studies. Several pilot-scale field studies also investigating the effect of HRT on nitrate removal or greenhouse gas production in bioreactors have used flow rates and porosity to estimate nominal HRT, similar to the procedure used in this study (Lepine et al., 2016; Hassanpour et al., 2017; Davis et al., 2019; Martin et al., 2019). Additionally, a number of laboratory column studies with similar objectives implemented the same approach as we used (Greenan et al., 2009; Christianson et al., 2017b; Bock et al., 2018a; Soupir et al., 2018). A study reported by Martin et al. (2019) found that HRT estimated using flow and porosity (2.1 ± 0.3 h) compared well with HRT estimated using bromide tracer (2.3 ± 0.3 h), and the authors opted to use the nominal HRT in their investigations.

2.4.3. Nitrate removal efficiency

The removal efficiency (RE) was calculated by dividing the difference of the cumulative inflow and outflow loads by the cumulative inflow load (Christianson et al., 2017b) for a specified period of time. Cumulative load was calculated by summing incremental loads, which were calculated as the product of the average of two consecutive concentration measurements and the flow volume within this period. The outlet flow data was used to calculate the flow volume of both the inflow and outflow (Goeller et al., 2019).

2.4.4. Nitrate removal rate

Many of the removal rates (RR) reported have been calculated for bioreactors where the through flow was regulated and therefore more

uniform (Greenan et al., 2009; Hoover et al., 2016; Lepine et al., 2016; Soupir et al., 2018; Martin et al., 2019). Our highly variable flows through the bioreactor pose a challenge for RR calculations, as the variable residence times make it difficult to identify the correct outflow water volume that needs to be compared to a given inflow volume. This difficulty is exacerbated by the fact that instantaneous inlet flow was not measured. To overcome this challenge, we decided to calculate the RR for periods sufficiently long so as to be not substantially affected by the varying inflow and outflow dynamics. Thus, the RR of the bioreactor was calculated as:

$$RR = \frac{R_N}{V_s\, t} \quad (2)$$

where R_N is the mass of nitrate-N removed from the drainage water (g), V_s is the saturated volume of the bioreactor (m^3), and t is the residence time (day) in the bioreactor of the volume of water for which the nitrate-N removal is determined. We selected a period of approximately half a month, which is about three times the average residence time for the 2018 season. Accordingly, the mass of nitrate-N removed (R_N) was determined from the difference of cumulative nitrate-N load at the inflow and outflow during the period, and t is the number of days during this period.

2.5. Statistical analysis

We used t-test to compare inflow and outflow results in order to determine the effect of bioreactor on drainage water quality. We used regression analysis to determine the relationship between two parameters in order to explain the factors influencing the performance of the bioreactor. Both statistical methods were done in MS Excel.

3. Results and discussion

3.1. Flow and hydrochemistry

Drainage flows through the bioreactor varied significantly between the two drainage seasons, with cumulative flows of 337 m^3 and 952 m^3 measured in part of 2017 (106 days) due to construction and in 2018 (124 days), respectively (Table 1). While the total rainfalls during the bioreactor operation were similar for both monitoring periods (Table 1), the smaller bioreactor flow in 2017 was due to fine sediments and biofilms clogging the header filter sock, which was installed around the distribution header in order to prevent small woodchips from entering and clogging the header. The filter sock was removed and the distribution header modified during the summer period between drainage seasons, resulting in unimpeded flow through the bioreactor in the 2018 season. While the peak flow during the 2017 season was only about 20 L min^{-1}, it was approximately 70 L min^{-1} in 2018 (Fig.4a). The average hydraulic residence time (HRT) was 21.1 days in 2017, and reduced to 4.7 days in 2018.

The subsurface inlet drainage water was found to have lowered oxygen but still aerated condition, with median dissolved oxygen (O_2) concentrations 3.2 and 4.7 mg L^{-1} measured at the bioreactor inlet during the two drainage seasons, respectively (Tables 2 and 3). In contrast, O_2 concentrations at the outlet were low (2017: 0.1–0.9 mg L^{-1}; 2018: 0.0–0.2 mg L^{-1}; Tables 2 and 3), indicating reduced conditions were established in the bioreactor suitable for denitrification. Threshold O_2 concentrations for the denitrification to occur are of the order 1 or 2 mg L^{-1} (Rivas et al., 2017; Stenger et al., 2018). Reduced conditions occurred at least from the middle of the bioreactor to the outflow, as O_2 measured in the 2018 drainage season in the well installed at the mid-distance along the bioreactor varied from 0 to 0.54 mg L^{-1} (data not shown).

Nitrate-N concentrations typical for subsurface drainage under intensive dairy farming (Tanner et al., 2003; Eckard et al., 2004) were measured in the inflow to the bioreactor, with a trend for declining concentrations with time observed in both drainage seasons (Table 2 and Fig. 4b). In 2017, the mean nitrate-N concentration was 5.59 (± 1.85) mg L^{-1}, whereas in 2018, the mean nitrate concentration was 13.72 (± 3.62) mg L^{-1}. The lower and less variable nitrate-N concentrations measured in 2017 can be explained by the early parts of the drainage season being missing in this time series. However, year-to-year variation is also evident, as almost all concentrations measured in 2017 were lower than the minimum concentration measured in 2018 (Fig. 4b). While flow peaks in the drainage (Fig. 4a) resulted in concurrent nitrate-N concentration peaks (Fig. 4b), there was a general trend of declining inflow nitrate-N concentrations with time (best-fitted to an exponential regression with R^2 of 0.76 and 0.77 for 2017 and 2018, respectively). Outflow nitrate-N concentrations were consistently and significantly lower ($p < .01$) with mean concentrations of 0.01 and 7.45 mg L^{-1} in 2017 and 2018, respectively. While the outflow concentration range was extremely narrow and near the analytical detection limit in 2017 (< 0.001–0.02 mg L^{-1}), the range was substantially wider in 2018 (< 0.001–16.40 mg L^{-1}) and strongly reflected the observed inflow peaks occurring at the higher flow rates (Fig. 4b).

The concentrations of dissolved heavy metals (arsenic, cadmium, chromium, copper and lead) were generally below detection limits both in the inflow and outflow during the two drainage seasons (data not shown). This indicates the low potential of the woodchip bioreactor to contaminate receiving open drains or streams with these metals. The concentrations of dissolved iron (Fe) and manganese (Mn) were significantly higher (both $p < .001$) in the outflow than in the inflow in 2017 (Table 2). The same is true for dissolved Fe in 2018 ($p = .09$), but in this year there was no significant difference ($p = .80$) between concentrations of dissolved Mn in the inflow (0.166 ± 0.053 mg L^{-1}) and in the outflow (0.173 ± 0.067 mg L^{-1}) (Table 3).

3.2. Nitrate removal and determining factors

3.2.1. Removal efficiencies and removal rates

Removal of nitrate from the drainage water was evident in the consistently and significantly lower nitrate concentrations in the outflow compared to the inflow during the two drainage seasons (Fig. 4b). Based on the cumulative nitrate-N loads at the inlet and the outlet, the bioreactor removed 1.94 kg and 6.01 kg of nitrate-N in 2017 and 2018, respectively. This translates to removal efficiencies of > 99% and 48% for the drainage season monitored in 2017 and 2018, respectively

Table 1
Flow, nitrate loads, and nitrate removal efficiency at the Tatuanui bioreactor during the two drainage seasons (part of 2017, 2018).

Drainage year	Dates of operation	Cum. rainfall[a] (mm)	Cum. flow (m^3)	Cumulative Nitrate load (kg N)			Removal Eff. (%)
				Subsurface drainage delivery	Bioreactor inflow	Bioreactor outflow	
2017	31 Jul – 13 Nov	444	337	2.36	1.95	< 0.01	99.9
2018	24 May – 24 Sep	415	952	12.58	12.47	6.46	48.2

[a] Recorded rainfall within the dates of operation of the bioreactor.

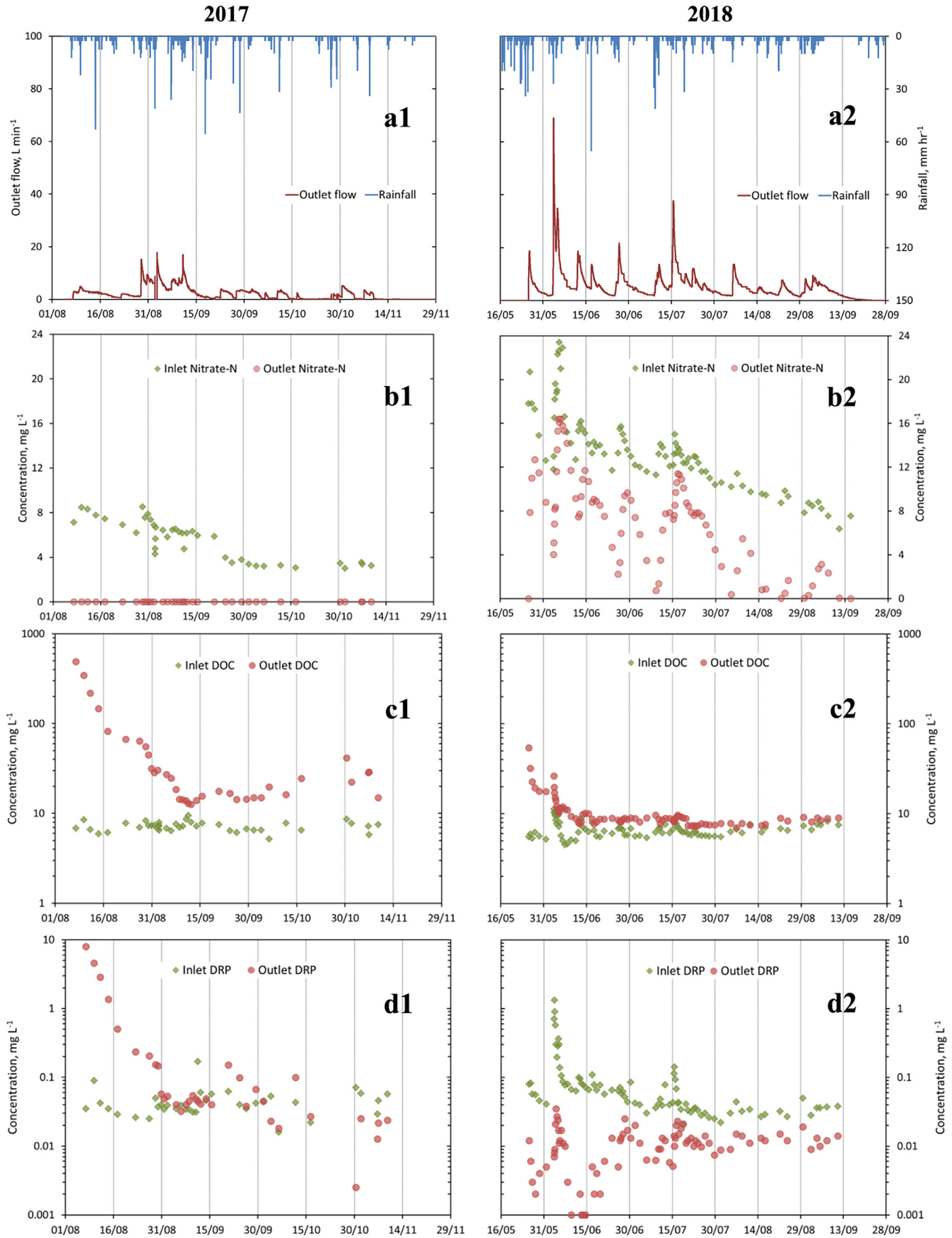

Fig. 4. Time series of (a) rainfall and flow at the bioreactor outlet, concentrations of (b) nitrate, (c) dissolved organic carbon (DOC), and (d) dissolved reactive phosphorus (DRP) in (1) 2017 and (2) 2018 drainage seasons.

Table 2
Statistics of selected water quality parameters in the inflow and outflow of the Tatuanui bioreactor during the 2017 drainage season.

Water Quality Parameter	Unit	Inflow						Outflow					
		Mean	Median	Min	Max	Std. dev	CV	Mean	Median	Min	Max	Std. dev	CV
O_2[a]	mg L^{-1}	3.6	3.2	2.1	6.3	1.3	35.7	0.6	0.6	0.1	0.9	0.2	39.2
pH[a]		5.6	5.5	5.4	6.0	0.2	3.9	5.6	5.7	4.9	6.0	0.4	6.3
EC[b]	µS cm^{-1}	449	448	209	528	34	7.5	434	411	115	912	102	23.5
Temp[b]	°C	13.3	12.9	10.0	15.5	1.1	8.2	13.4	13.2	11.2	15.8	0.7	5.4
NO_3-N	mg L^{-1}	5.59	13.20	3.00	8.52	1.85	33.1	0.01	0.01	< 0.001	0.02	0.01	91.2
NH_4-N	mg L^{-1}	0.100	0.071	0.037	0.375	0.079	79.2	0.278	0.018	0.005	2.233	0.56	202.7
TN	mg L^{-1}	6.37	6.90	3.81	9.25	1.78	28.0	2.01	1.45	0.91	9.69	1.81	89.9
DRP	mg L^{-1}	0.045	0.040	0.016	0.170	0.026	56.8	0.533	0.049	0.003	7.940	1.549	290.7
TP	mg L^{-1}	0.072	0.062	0.027	0.333	0.049	68.2	0.659	0.156	0.062	9.180	1.764	267.7
DOC	mg L^{-1}	7.16	7.20	5.20	9.50	0.90	12.6	57.18	23.40	12.60	491.00	99.14	173.4
SO_4^{2-}	mg L^{-1}	116.1	120.0	80.0	140.0	12.9	11.1	46.5	46.0	8.5	91.0	29.1	62.5
N_2O[a]	µg L^{-1}	36.3	38.3	11.3	58.6	14.5	39.8	5.9	3.0	0.2	20.4	7.8	132.7
CH_4[a]	µg L^{-1}	24.1	15.1	< 0.01	15.1	24.9	103.2	2145.7	1681.5	638.2	4500.0	1387.5	64.7
Fe	mg L^{-1}	0.054	0.015	< 0.0007	0.339	0.092	170.8	0.971	0.666	0.066	3.461	0.908	93.4
Mn	mg L^{-1}	0.140	0.127	0.066	0.276	0.049	34.6	0.862	0.645	0.003	2.240	0.725	84.1

CV – coefficient of variation; O_2 – dissolved oxygen; EC – electrical conductivity; Temp – temperature; TN – total nitrogen; DRP – dissolved reactive phosphorus; TP – total phosphorus; DOC – dissolved organic carbon; Fe – dissolved iron; Mn – dissolved manganese.
Unless indicated, water quality parameters were measured from water samples collected automatically.
[a] Measured from samples collected manually or measured in situ during the collection of manual samples.
[b] From real time data monitored every five minutes (during the operational period).

(Table 1). The smaller nitrate-N mass removed in 2017 was due to the limited flow through the bioreactor due to the clogging of the header. The removal efficiency of the Tatuanui bioreactor in 2018 was in the middle to upper range of values (12–76%) reported in other studies (Christianson et al., 2017b; Roser et al., 2018).

The temporal variation of the removal efficiency (RE) within the 2018 drainage season is shown in Fig. 6; there was very little variation during 2017 due to the essentially complete nitrate removal throughout the monitored period of the drainage season. As discussed, the length of the period used for the calculations of incremental removal efficiencies was approximately 15 days (i.e. half-monthly). This period is approximately three times the average HRT (4.7 days) in the bioreactor during 2018, except for the first incremental period (May-I; 7-day period). We also computed the corresponding average HRT over the same period. Therefore, any inaccuracies of using flow and porosity in estimating HRT would have minimal effect on the succeeding analysis considering the variability in the flow within each period. A very strong correlation was found between HRT and RE ($r = 0.97$, $p < .001$, Fig. 7a). The lowest nitrate removal efficiency (31%) was observed in the second half of July (Jul-II) with the lowest HRT of 2.8 days, whereas the highest efficiency (93%) was observed in the second half of August (Aug-II) when the HRT was 6.4 days (Fig. 6 and 7a). The strong exponential relationship between HRT and RE ($R^2 = 0.99$) indicates the dominant influence of HRT on nitrate removal in spite of other factors (e.g. electron donor, electron acceptor, temperature, etc.) also having an effect (David et al., 2016; Soupir et al., 2018). This close relationship between HRT and RE has also been reported in previous studies (Greenan et al., 2009; Weigelhofer and Hein, 2015; Hoover et al., 2016; Lepine et al., 2016; Hassanpour et al., 2017; Soupir et al., 2018; Martin et al., 2019). Using the K-fold leave-one-out cross validation method, Martin et al. (2019) quantified the dominant influence of HRT: 93% of RE attributed to HRT, the remainder attributed to nitrate inflow concentrations (6.2%), temperature (0.5%) and O_2 (0.2%). Extrapolation of the HRT-RE curve indicates that an essentially complete removal of

Table 3
Statistics of selected water quality parameters in the inflow and outflow of the Tatuanui bioreactor during the 2018 drainage season.

Water Quality Parameter	Unit	Inflow						Outflow					
		Mean	Median	Min	Max	Std. dev	CV	Mean	Median	Min	Max	Std. dev	CV
O_2[a]	mg L^{-1}	4.7	4.7	2.6	6.6	1.4	30.1	0.0	0.0	0.0	0.2	0.1	230.0
pH		6.7	6.7	5.7	7.8	0.4	5.4	7.1	7.2	6.0	7.7	0.4	6.2
EC[b]	µS cm^{-1}	512	520	308	690	34	6.7	491	504	353	552	43	8.7
Temp[b]	°C	12.3	11.9	11.1	14.9	0.8	6.6	12.9	12.4	11.6	19.8	1.3	9.8
NO_3-N	mg L^{-1}	13.72	13.20	6.38	23.40	3.62	26.4	7.45	7.75	< 0.001	16.40	4.38	58.8
NH_4-N	mg L^{-1}	0.151	0.091	0.038	0.907	0.158	104.9	0.096	0.075	0.012	0.329	0.063	65.7
TN	mg L^{-1}	14.54	14.50	7.14	21.74	3.38	23.2	8.57	8.57	0.80	18.65	4.56	53.2
DRP	mg L^{-1}	0.109	0.054	0.021	1.330	0.195	178.8	0.011	0.011	0.001	0.035	0.007	61.2
TP	mg L^{-1}	0.162	0.080	0.034	1.860	0.274	168.9	0.050	0.032	0.019	0.315	0.052	105.1
DOC	mg L^{-1}	6.76	6.45	4.50	11.30	1.35	19.9	10.66	8.80	7.00	53.90	6.39	60.0
SO_4^{2-}	mg L^{-1}	101.3	100.0	34.0	150.0	21.0	20.8	99.9	100.0	69.0	130.0	14.4	14.4
N_2O[a]	µg L^{-1}	50.8	45.3	26.8	83.0	17.0	33.4	92.0	39.6	0.6	306.4	100.1	108.8
CH_4[a]	µg L^{-1}	3.3	2.5	1.0	7.5	2.1	64.5	73.6	50.3	15.0	307.4	90.6	123.0
Fe	mg L^{-1}	0.022	0.012	0.005	0.055	0.019	85.9	0.219	0.069	0.011	0.974	0.326	148.8
Mn	mg L^{-1}	0.166	0.166	0.081	0.260	0.053	31.8	0.173	0.136	0.110	0.271	0.067	38.9

CV – coefficient of variation; O_2 – dissolved oxygen; EC – electrical conductivity; Temp – temperature; TN – total nitrogen; DRP – dissolved reactive phosphorus; TP – total phosphorus; DOC – dissolved organic carbon.
Unless indicated, water quality parameters were measured from water samples collected automatically.
[a] Measured from samples collected manually or measured in situ during the collection of manual samples.
[b] From real time data monitored every five minutes (during the operational period).

nitrate-N at our site conditions may be expected with a residence time of 6.7 days. In agricultural lands in north-eastern USA, in smaller bioreactors with an average bioreactor volume of 10.8 m^3, it has been reported that the required HRT to achieve a 100% RE ranges from 0.36 to 2.96 days (Hassanpour et al., 2017). This translates, for these conditions, to a woodchip volume of between 3.7 and 30 m^3 per day required to achieve 100% N removal. Using this result, and our 56.3 m^3 of woodchip, we would require a HRT of between 1.9 and 15.2 days to provide similar amount of exposure to woodchip material for complete nitrate removal, the mid-point of which corresponds with our estimate of 6.7 days. While other studies investigated the relationship between nitrate removal and HRT (Greenan et al., 2009; Martin et al., 2019) or inflow nitrate-N concentrations (Hoover et al., 2016; Nordström and Herbert, 2019), these studies applied controlled flow system. We, therefore, opted to investigate the relationship between RE with inflow N-load to represent the changes in substrate load given the variability of flow and concentrations at our site. We found a strong negative power relationship between inflow nitrate-N load and RE (Fig. 8a; r = -0.80; p = .02). This result is in contrast to the positive relationship observed in other studies where inflows were controlled and uniform (Martin et al., 2019). In our work this result may be attributed to the dynamic flow at the site, with observed high nitrate concentrations during high flows resulting in shorter residence times at the higher nitrate loads (Fig. 7b; r = 0.72, p = .04).

The highest removal rate (RR), which is the mass removal per unit volume of bioreactor per unit time, was observed in the first half of June (Jun-I; austral winter) and the lowest at the end of the drainage season in the first half of September (Sep−I) (Fig. 6). We found that inflow nitrate-N load had a significant positive influence on RR (Fig. 8b). The strong positive relationship between inflow nitrate-N load and RR (r = 0.82, p = .01) indicates the positive effects of substrate load. Other studies have also highlighted the influence of substrate load (in terms of nitrate concentrations for controlled flow conditions) on RR (Griessmeier et al., 2019; Nordström and Herbert, 2019).

No realistic RR could be computed for the 2017 drainage season due to the extremely low nitrate concentrations in the outflow (mean $<$ 0.01 mg N L^{-1}). Such low outflow concentrations reflect that denitrification was limited by insufficient nitrate-N availability within the bioreactor. Accordingly, any calculated RR would only represent a minimum that was achieved. In 2018, the computed RR for the same periods as used for the RE reported above varied between 0.67 and 1.60 g N m^{-3} day^{-1} (Fig. 6). This range is within the 0.38–3.78 g N m^{-3} day^{-1} range reported for field-scale bioreactors installed in Iowa (USA) (Jaynes et al., 2008; Christianson et al., 2012b), and also comparable to RR of $<$ 1 g N m^{-3} day^{-1} observed in a woodchip bioreactor with 10% (v/v) biochar in Virginia (USA) (Bock et al., 2018b).

As mentioned previously in the context of the 2017 data, nitrate RR are underestimated when a nitrate-N limitation occurs within the bioreactor, as indicated by outflow concentrations near the detection limit. However, there is some uncertainty about which threshold concentration indicates N limitation conditions. For instance, in denitrification studies in general (i.e. not limited to woodchip bioreactors), Tchobanoglous et al. (2014) posited that nitrate reduction is limited by the nitrate concentrations only at concentrations below 0.02 to 0.05 mg of NO_3-N L^{-1}, much lower than the threshold of 0.23 to 0.34 mg of NO_3-N L^{-1} observed by Bowman and Focht (1974). In the 2018 drainage season, five outlet samples had nitrate concentrations at or below 0.05 mg NO_3-N L^{-1} observed during the periods May-I, Aug-II, and Sep−I. Thus, the estimated RR during these periods might have been underestimated and the half-monthly minimum RR at the Tatuanui bioreactor could be higher than 0.67 g N m^{-3} day^{-1}. Nonetheless, the relatively low number of observations of nitrate-N concentrations at the outlet below 0.05 mg NO_3-N L^{-1} (5.7%) does not significantly affect the representative range of RR presented here.

Temperature in the inflow water was not found to be correlated with either RE (r = −0.42, p = .30) or RR (r = 0.63, p = .10), indicating that temperature was not significantly affecting the nitrate removal properties of the bioreactor. This could be attributed to a narrow range of low temperatures during the 2018 drainage season (11.9–14.9 °C; Table 3), and consistent with other studies that found no apparent trend or relationship between temperature and RR at temperatures below 16 °C (Hassanpour et al., 2017).

Calculation of RR is helpful in terms of comparing how a specific bioreactor performs compared with other bioreactors. On the other hand, comparison should not be limited to RR alone, because as shown above, there are other factors (e.g. site-specific range of inflow nitrate concentrations) that will affect achievable RR. The more useful metric for performance assessment at a specific location may be the RE as it clearly shows the proportion of nitrate load removed from the drainage water. Both metrics, however, should be applied concurrently to ascertain and improve the performance of bioreactors.

3.2.2. Electron donor (organic carbon) availability

The differing availability of organic carbon (OC) in the bioreactor, indicated by the amount of dissolved organic carbon (DOC) in the outflow, can partly explain the difference in the nitrate removal efficiencies between the two drainage seasons. In 2017, approximately 18.1 kg DOC (318 mg C L^{-1} of bioreactor volume) was discharged at the outlet as compared to 9.3 kg DOC (165 mg C L^{-1}) in 2018, despite the greater flow through the bioreactor in 2018 (Fig. 4c and Fig. 9).

The total mass of DOC generated within the bioreactor was estimated from: the sum of cumulative DOC mass discharged at the outlet, plus the DOC mass consumed during denitrification, minus the cumulative DOC mass that entered the bioreactor with the drainage water at the inlet. Based on the stoichiometry of heterotrophic denitrification with carbon as the electron donor, 1.25 mmol C is required to denitrify 1.0 mmol of nitrate-N (Spalding and Parrot, 1994). Thus, the mass of DOC needed to account for the estimated nitrate-N removed were 2.10 kg and 6.46 kg in 2017 and 2018, respectively. The cumulative DOC masses that entered the bioreactor were 2.44 kg and 6.37 kg in 2017 and 2018, respectively. It is recognised that the DOC being leached from the soil probably has different bioavailability as to the carbon made available from the woodchip, which adds some uncertainty to these estimations of DOC. The amount of DOC required for aerobic respiration to lower the O_2 concentrations unfortunately, could not be reliably estimated due to the limited number of DO measurements (n = 9) both at the inlet and outlet. Nevertheless, the estimated total DOC made available from the woodchips, accounting for the DOC used for the mass of nitrate-N removed, were 17.75 kg (or 315 mg DOC L^{-1} of bioreactor volume) and 9.34 kg (or 166 mg DOC L^{-1}) for 2017 and 2018, respectively. For the entire operational period of the two drainage seasons, the amount of DOC consumed for the removal of nitrate accounted for 12% and 68% of woodchip-derived DOC for the 2017 and 2018 seasons, respectively, highlighting the greater DOC availability and lower nitrate load in 2017. The amount of DOC consumed for nitrate reduction accounted for 9.2% and 29% of total available DOC for the 2017 and 2018 seasons, respectively. While it is observed that in both seasons a significant amount of DOC was released in the early part of the season, the greater DOC available in 2017 than in 2018 with respect to nitrate-N was also indicated in the C/N ratio of the DOC discharged and nitrate-N entering the bioreactor. Excluding the period in 2017 when DOC release was high (at approximately 100 m^3 of flow through the bioreactor, Fig. 4c), the mean C/N ratio in 2017 (4.64 ± 2.53) was significantly higher (p $<$ .01) than in 2018 (0.79 ± 0.38). The greater availability of electron donor in 2017 was also indicated by sulphate reduction (Griessmeier et al., 2019) as discussed in a later section.

3.3. Secondary effects

3.3.1. DOC discharge

As shown in Fig. 4c, more DOC exited than entered the bioreactor as indicated by the consistently higher DOC concentrations in the outlet than in the inlet. However, it should be noted that approximately the first 100 m^3 of flow (Fig. 4c and Fig. 9), equivalent to 3 to 3.5 pore volumes of the bioreactor, accounted in both years for a very high fraction of the increased DOC discharges. The big initial DOC flushed during the start-up of the bioreactor in 2017, which may be due to easily leachable tannic acids in fresh woodchips (Schipper et al., 2010), accounted for approximately 74% of the total DOC discharge during this season. A smaller initial flush in 2018 accounted for approximately 21% of the total DOC discharge. This initial flush in the 2018 season could be attributed to the breakdown of aerated woodchips (Maxwell et al., 2019) as the bioreactor was drained during the non-operational summer period to avoid strongly reduced condition causing 'rotten egg' smell.

3.3.2. Release and retention of phosphorus

We observed an increased discharge of dissolved reactive phosphorus (DRP) from the Tatuanui bioreactor during most of the 2017 drainage season, but DRP retention occurred throughout the entire 2018 drainage season. In 2017, an initial flush of DRP was observed up to the end of August 2017 accounting for 93% of DRP released from the bioreactor during the season (Fig. 4 d1). A total of 15 g DRP entered the bioreactor, whereas a total of 155 g of DRP exited the bioreactor. This high release of DRP at the early stage of operation of a woodchip bioreactor was also observed in other studies (Healy et al., 2015; Fenton et al., 2016; von Ahnen et al., 2016; Husk et al., 2018). After this initial flush, outflow DRP concentrations were mostly moderately enhanced compared to inflow concentrations. However, towards the end of the season (from late October), DRP retention was observed with lower concentrations in the outflow than in the inflow.

The retention of DRP in the bioreactor continued throughout the 2018 season with consistently lower DRP concentrations observed in the outflow (0.01 ± 0.01 mg L^{-1}) compared to the inflow (0.11 ± 0.19 mg L^{-1}). DRP concentrations in the outflow were reduced to a level below the Australian and New Zealand Environment and Conservation Council (ANZECC) 2000 water quality guideline of long-term irrigation trigger value of 0.05 mg L^{-1} to minimise algal growth. Approximately 95 g DRP entered the bioreactor and only 10 g DRP exited from the bioreactor, representing approximately 89% removal of DRP from the drainage water. This observed DRP removal was unexpected as limited data in the literature seemed to highlight the release of DRP (Herbstritt, 2014; Healy et al., 2015; Weigelhofer and Hein, 2015; David et al., 2016; Fenton et al., 2016) especially at the early stage of bioreactor operations. Moreover, several authors proposed modifications of woodchip bioreactors (e.g., adding P adsorbent materials) for phosphorus removal (Zoski et al., 2013; Bock et al., 2016; Gottschall et al., 2016; Hua et al., 2016; Christianson et al., 2017b). While no specific reasons were given, it was apparently assumed that woodchips bioreactors have no or insufficient P removal capacity. In addition, woodchips have not been listed as useful substrate for phosphorus removal in published reviews (Johansson Westholm, 2006; Vohla et al., 2011), probably due to the lack of data of the removal properties of woodchips. However, a few studies also reported significant reduction (35–53%) in total P (TP) by woodchip bioreactors, though mainly attributed to removal of particulate P rather than dissolved P (Choudhury et al., 2016; Robertson et al., 2018). At the Tatuanui bioreactor, TP removal was 68% in 2018. A very limited number of studies showed DRP removal by woodchips at a much lower removal efficiency (< 10–53%) in columns or small bioreactors (< 2 m^3) (Goodwin et al., 2015; Sharrer et al., 2016), and field-scale bioreactors (16–33 m^3) (Choudhury et al., 2016; Husk et al., 2018). The reasonably long average HRT of 4.7 days of drainage water in the Tatuanui bioreactor in 2018 might have contributed as DRP removal seemed apparent when HRT is longer (e.g., 42–55 h in 1.76 m^3 bioreactors) (Sharrer et al., 2016).

As discussed above, this DRP removal in the Tatuanui bioreactor was first detectable in the later part of the 2017 drainage season when DRP concentrations in the outflow (0.0025–0.025 mg L^{-1}) were lower than in the inflow (0.029–0.071 mg L^{-1}) (n = 5), from the 91st day of the operation (30 Oct – 11 Nov) (Fig. 4d). Similar reversal from DRP release in the early stages of operation to DRP removal (28–53%) was also observed in other bioreactors (Sharrer et al., 2016; Husk et al., 2018). However, DRP removal was not observed in other bioreactor studies running for similar periods (David et al., 2016; Fenton et al., 2016). Thus, continued monitoring of DRP concentrations over multiple seasons would be essential to confirm the longer term DRP removal potential of woodchip bioreactors. However, this was outside the scope of this study. Considering that several mechanisms, such as adsorption, immobilisation, precipitation, etc., could be responsible for the removal of DRP from drainage water (Bock et al., 2015; Husk et al., 2018; Carstensen et al., 2019), further studies outside the scope of this paper are needed to understand the dynamics and factors determining removal due to different outcomes observed in investigations of woodchip bioreactors. For instance, precipitation of the DRP out of solution seems not a significant removal mechanism in the Tatuanui bioreactor. This is reflected in the observed 68% TP removal in 2018, assuming precipitated DRP remained as suspended particulates.

While an initial DOC flush was observed in the early part of the 2018 season (May to early June), this was not the case for DRP. In contrast, greater DRP removal was observed during this period as indicated by the greater difference between inflow and outflow concentrations (Fig. 4 d2). This could suggest that, as a consequence of the draining of the bioreactor at the end of the previous drainage season, the release of the organic matter from the woodchips during the early stage (due to the partial breakdown of woodchips) (Fig. 4 c2) may have provided new adsorption sites for DRP retention. This was not observed in the early part of 2017 where an initial flush of both DOC and DRP was observed due to the fresh conditions of the woodchips. Noting the high initial flush of both DOC and DRP during the start-up phase of bioreactor operation, as observed in other studies, it is recommended that initial discharges from bioreactors with fresh woodchips (approximately the first 3 to 3.5 pore volumes) be applied to land instead of being discharged to streams or open drains.

3.3.3. Nitrous oxide concentrations

In 2017, N_2O concentrations in the drainage water entering the bioreactor were on average 36.3 (± 14.5) μg N_2O L^{-1} (Fig. 5 b1), which was substantially higher than concentrations in drainage water observed by Davis et al. (2019). The lowest observed concentration of 11.3 μg N_2O L^{-1} was still substantially higher than the equilibrium concentration of 0.35 μg N_2O L^{-1} with the atmosphere at 20 °C (Jurado et al., 2017). The elevated N_2O concentrations in the inflow indicated N_2O production in the pastoral soil-water system, likely due to nitrification given the prevailing oxic conditions, presence of elevated nitrate, and of ammonium – in terms of ammoniacal N (2017: 0.10 ± 0.08 mg N L^{-1}; 2018: 0.15 ± 0.16 mg N L^{-1}) with slightly acidic pH (2017: 5.6 ± 0.2; 2018: 6.7 ± 0.4) (Tables 2 and 3). However, N_2O concentrations in the outflow were significantly lower (p < .01) with a mean of 5.9 (± 7.8) μg N_2O L^{-1}. It is apparent from this decrease in the N_2O concentrations that the conditions within the bioreactor favoured complete denitrification to dinitrogen gas (N_2).

In 2018, the average N_2O concentrations in the inflow (50.8 ± 17.0 μg N_2O L^{-1}) and outflow (92.0 ± 100.1 μg N_2O L^{-1}) were not significantly different (p = .24), but there was a clear temporal variation. During the first half of the season (1 June – 20 July), it is apparent that N_2O concentrations in the outflow (179.68 ± 88.76 μg N_2O L^{-1}) were higher than in the inflow (61.14 ± 15.84 μg N_2O L^{-1}). During this period, the mean HRT of the drainage water in the

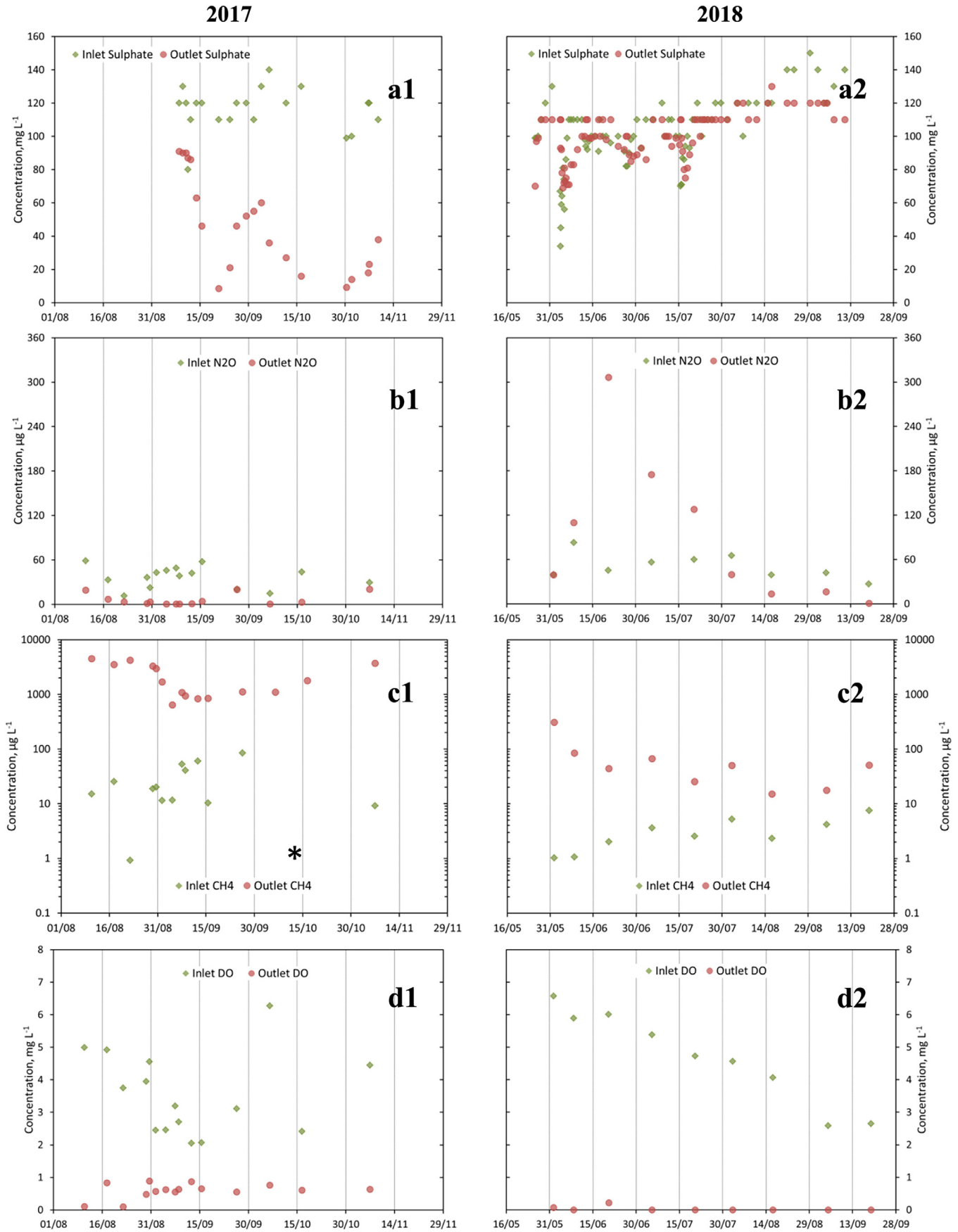

Fig. 5. Time series of concentrations of (a) sulphate, (b) dissolved nitrous oxide (N_2O), (c) dissolved methane (CH_4), and (d) dissolved oxygen (DO) in (1) 2017 and (2) 2018 drainage seasons. *CH_4 not detected in water samples collected from the inlet in early-mid October 2017 (c1).

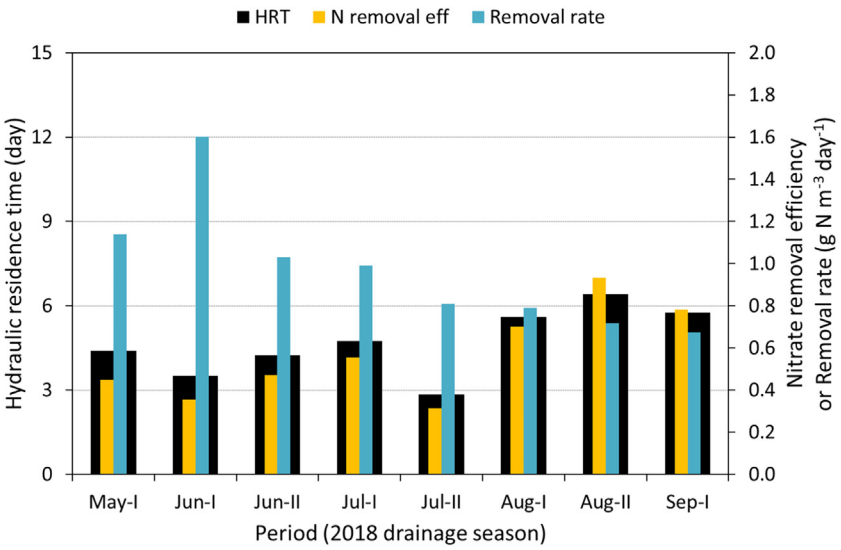

Fig. 6. Time series of half-monthly average hydraulic residence time (HRT), nitrate removal efficiency, and removal rates during the 2018 drainage season. Roman numbers I and II on the x-axis label refer to the first and second half periods of the month.

bioreactor was 3.9 days. In the latter half of the season (20 July – 19 Sep), on the other hand, the mean HRT of the drainage water was nearly double at 7.4 days and the N_2O concentrations in the outflow (17.55 ± 16.24 μg N_2O L^{-1}) were lower than in the inflow (43.30 ± 15.99 μg N_2O L^{-1}) (this estimated HRT does not exactly match with Fig. 6 due to the different period covered: automatically collected samples ended on 15 Sep, whereas manually collected samples for dissolved gases ended on 19 Sep). The shorter HRT in the earlier half of the drainage season may have contributed to the incomplete denitrification process in some instances within the bioreactor resulting in N_2O being the terminal product instead of the benign N_2 gas; hence the higher N_2O concentrations in the outflow. Moreover, the higher nitrate concentrations in the subsurface drainage during this early part of the drainage season (14.9 ± 3.1 vs 10.0 ± 1.8 mg NO_3-N L^{-1} in the latter half of the season) may also have contributed to the incomplete nitrate reduction process (Elgood et al., 2010), as more available carbon and/or a longer HRT would have been required for complete reduction of this enhanced nitrate load (Griessmeier et al., 2019). It is less likely that the incomplete denitrification process was due to a lack of N_2O reductase, the enzyme that catalyses the reduction of N_2O to N_2. The reason being that more complete reduction was observed in the later part of the 2018 drainage season as well as during the previous drainage season, and woodchips have been found to contain diverse microbial communities including those with N_2O reductase (Nos) enzymes (Griessmeier et al., 2019).

While N_2O emissions were not measured in this study, it has been found that N_2O emission from the surface of bioreactors were no greater than emissions from agricultural soils (Elgood et al., 2010; Goeller et al., 2019) and found to be less than 1% of the nitrate removed (David et al., 2016). Moreover, N_2O production in bioreactors (both emitted on the surface and dissolved in the outflow water) had been found to be only < 0.4 to 5.2% of nitrate consumed (Elgood et al., 2010; Christianson et al., 2013a; Davis et al., 2019). Additionally, the soil cover of approximately 0.50 m on top of the woodchips is likely to mitigate any N_2O emissions from the woodchips before they could reach the atmosphere. Even thin soil covers (0.05 m) were reported to result in lower N_2O fluxes compared to woodchips alone in lab-scale bioreactors (Christianson et al., 2013a). The reduced emissions under a soil cover could be due to the capability of the soil microorganisms to mitigate N_2O, as well as the soil layer's capping effect that constrains upward gas flux, thereby providing more opportunity for the gas to remain dissolved in the drainage water and discharged in the outflow (Christianson et al., 2013a).

3.3.4. Sulphate reduction

Following the thermodynamic sequence of electron acceptors (Rivett et al., 2008), sulphate reduction can be expected in conditions with low availability of less reduced electron acceptor such as oxygen and nitrate (Lepine et al., 2016). On the other hand, given the supply of organic carbon (electron donor) from the woodchips, HRT influences the availability of oxygen and nitrate. This is reflected in the strong positive relationship between HRT and RE (Fig. 7a), indicating that at longer HRT less nitrate (and oxygen) is available. Thus, the long HRTs typical for the 2017 drainage season induced sulphate reduction in the bioreactor. This was evident in the substantially higher (p < .01) sulphate concentrations in the inflow (116.1 ± 12.9 mg L^{-1}) than in the outflow (46.5 ± 29.1 mg L^{-1}) in 2017 (Fig. 5 a1). While hydrogen sulphide (H_2S) was not measured, the decrease in sulphate concentration corresponded to the production of H_2S, an odorous gas easily detected due to its characteristic rotten egg smell. This smell was observed at the site especially during periods with very low flows (i.e. long HRTs). Long HRTs resulted in highly reduced conditions in the drainage water, indicated by the very low or negligible amount of nitrate in the outflow (0.01 ± 0.01 mg L^{-1}) and significantly higher concentrations of dissolved Fe and Mn in the outflow than in the inflow (Table 2). This sulphate reduction during long HRT has also been observed in other bioreactor studies (Lepine et al., 2016; Christianson et al., 2018; Carstensen et al., 2019).

In contrast, the shorter HRTs observed in 2018 resulted in comparable (p = .60) mean sulphate concentrations in the inflow (101.3 ± 21.0 mg L^{-1}) and the outflow (99.9 ± 14.4 mg L^{-1}) (Table 3), indicating that overall H_2S production was insignificant. However, closer scrutiny over the season revealed periods in which sulphate reduction occurred, although to a much lesser extent than in 2017 (Fig. 5a). Concurrent measurements of inflow and outflow concentrations indicated that sulphate reduction occurred in periods with average HRTs ranging from 3.0 to 7.6 days. The most obvious period was in the later part of the season (21 Aug – 11 Sep), in which the average HRT was 5 days and significantly different concentrations (p < .01) were observed in the inflow (135.0 ± 10.7 mg L^{-1}) and in the outflow (117.5 ± 4.6 mg L^{-1}). On the other hand, the average HRTs during which we observed no significant difference in sulphate concentrations, or the outflow concentrations were even higher, ranged from 0.7 to 4.7 days. The overlapping HRT ranges (no reduction at

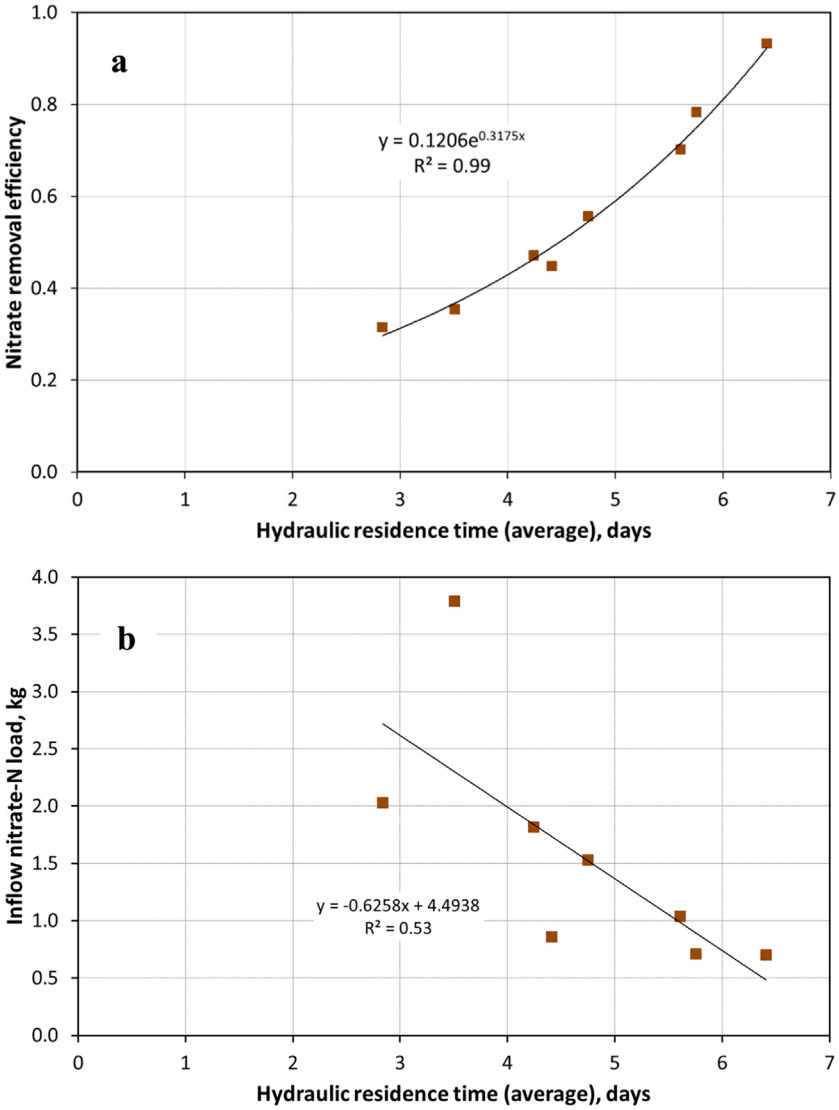

Fig. 7. Relationship between hydraulic residence time (HRT) and (a) nitrate removal efficiency and (b) inflow nitrate-N load to the bioreactor during the 2018 drainage season.

0.7–4.7 days vs. with reduction at 3–7.6 days) demonstrates that HRT is not the only factor determining the reduction of sulphate in the bioreactor. The variable inflow nitrate-N concentrations or nitrate-N loads may have influenced the overlapping HRT ranges for the observed with or without sulphate reduction. This is due to the variable HRTs needed to lower nitrate concentrations to conditions conducive for sulphate reduction. This seemed to be the case in some instances in which we observed sulphate reduction (Fig. 5 a2) when nitrate concentrations in the outflow were very low (Fig. 4 b2). On the other hand, sulphate reduction may still occur even if substantial nitrate is still present in the bioreactor. This is due to spatial variability in redox status within the bioreactor (e.g. microsites), as discussed below with regard methane production.

3.3.5. *Methane production*

Methanogenesis (or methane production) was observed in the Tatuanui bioreactor during both drainage seasons although to a significantly different extent (Fig. 5c). In the 2017 drainage season, mean CH_4 concentration in the outflow (2146 ± 1388 μg L^{-1}) was nearly 90 times the mean concentration in the inflow (24 ± 24 μg L^{-1}). In 2018, mean concentration in the outflow (74 ± 91 μg L^{-1}) was still significantly higher than in the inflow (3 ± 2 μg L^{-1}), however much lower than in the 2017 outflow. It is apparent that the highly reduced conditions in the bioreactor during 2017, indicated by the very low O_2 (0.6 ± 0.2 mg L^{-1}) and nitrate (0.01 ± 0.01 mg N L^{-1}) (Fig. 5d and 4b) and higher dissolved Fe and Mn (Table 2) concentrations in the outflow, resulted in the substantial production of methane as previously described by (Elgood et al., 2010). While substantial nitrate-N concentrations were still measured in the outflow in 2018 (7.45 ± 4.38 mg N L^{-1}), the reduced condition in the bioreactor indicated by the low O_2 concentrations (0 ± 0.1 mg L^{-1}) (Fig. 5d) and higher dissolved Fe concentrations (Table 3) measured in the outlet provided a conducive environment for some CH_4 production, although at only about 3.5% of the 2017 levels. The lower rate in 2018 could be attributed to the shorter HRT, as HRT has been shown to positively affect methane production (Davis et al., 2019). These results indicate that methanogenesis may occur simultaneously with nitrate reduction as long as there are reduced conditions and organic carbon is available, particularly when HRT is high. This is also demonstrated in the early part of 2018 when higher methane concentrations were observed in the outflow, which could be largely attributed to the abundance of organic carbon in the bioreactor (Fig. 4 c2) and the long HRT (8.4 days). The simultaneous occurrence of the two processes has been attributed to the spatial distribution in the bioreactor of the microorganisms responsible

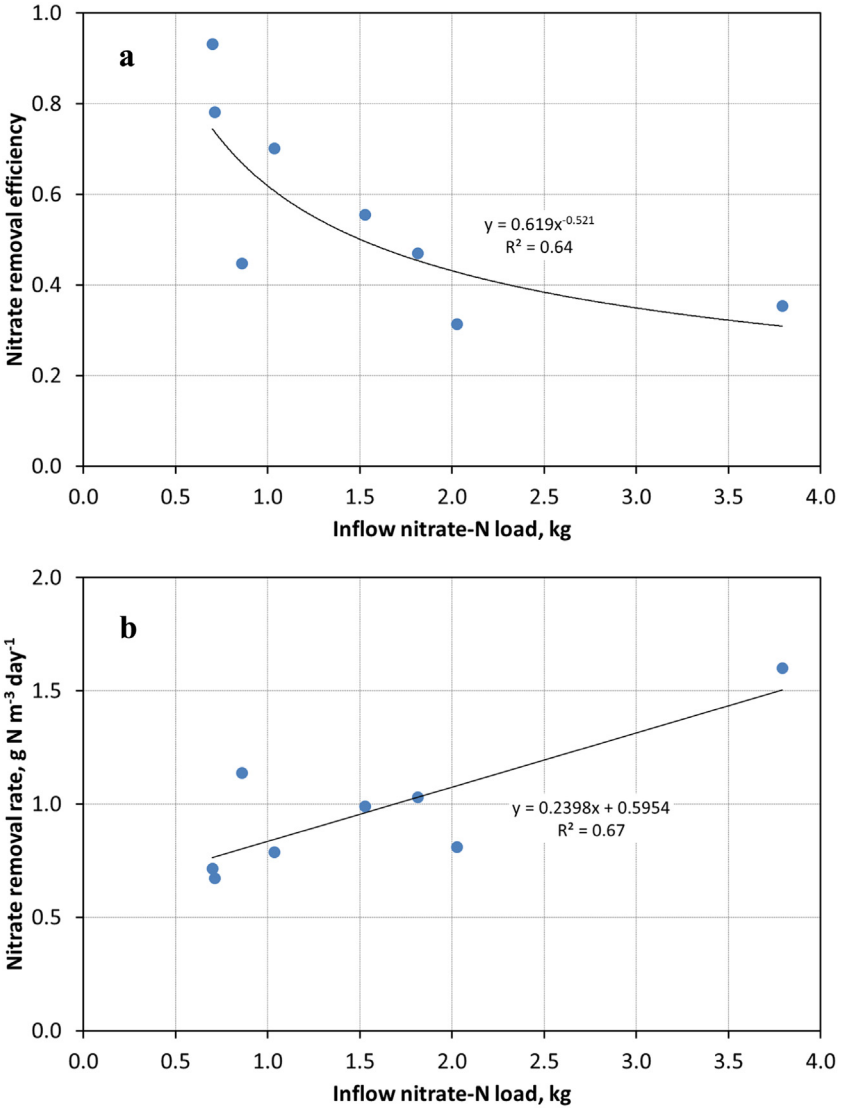

Fig. 8. Relationship between inflow nitrate-N load and nitrate (a) removal efficiency and (b) removal rate in the bioreactor during the 2018 drainage season.

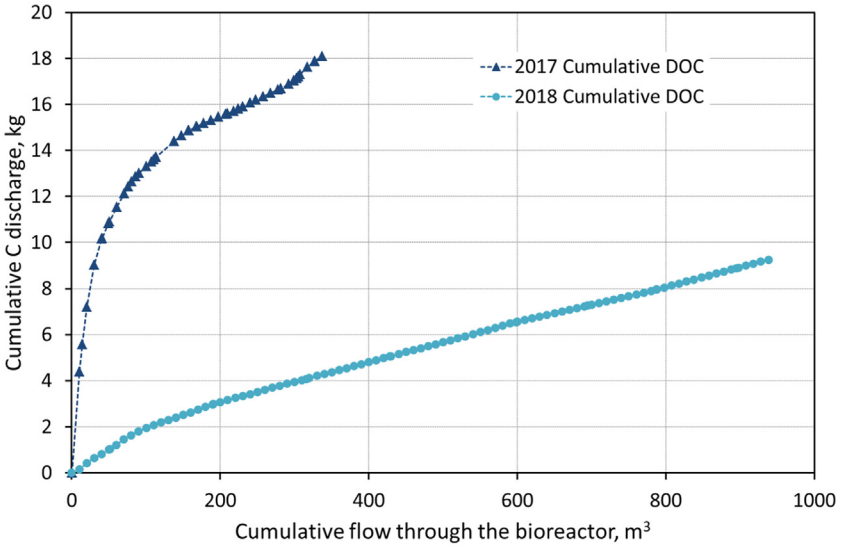

Fig. 9. Cumulative dissolved organic carbon (DOC) discharged from the bioreactor against cumulative flow through the bioreactor in 2017 and 2018.

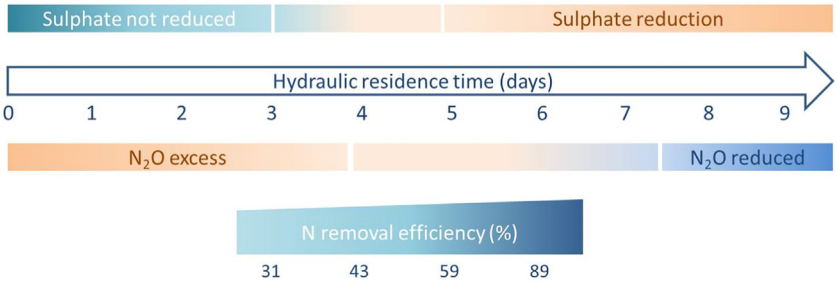

Fig. 10. Relationship of hydraulic residence time (HRT) with nitrate removal efficiency, sulphate reduction (indicating H_2S production), and N_2O production (incomplete denitrification process) derived from the Tatuanui bioreactor data. Periods of HRT range without label indicate possible transition between reduction and no reduction of sulphate or N_2O. Removal efficiencies were derived from Fig. 7a and scale matching the HRT scale.

for the two processes (Griessmeier et al., 2019) and/or different redox status at different microsites or hot spots (e.g. driven by differing hydraulic properties or non-equilibrium solute transport) (Carstensen et al., 2019; Davis et al., 2019).

3.4. Implications for bioreactor optimisation to enhance nitrate removal while minimising negative secondary effects

The ideal operation of a woodchip bioreactor would be to maximise nitrate removal without any undesirable side effects. This study observed that hydraulic residence time (HRT) has a significant influence on both the removal of nitrate and the production of greenhouse (N_2O and CH_4) and odorous gases (H_2S). Short HRT (< 3 days) were required to avoid sulphate reduction (and therefore, H_2S production). However, encouraging complete reduction of nitrate and avoiding excess N_2O in the discharge required longer HRT (> 7.5 days) (Fig. 10). There seems to be a potential HRT range of between 4 and 5 days in the Tatuanui bioreactor in which the production of both H_2S and N_2O could be minimised. This range of HRT is longer than 2.2–2.9 days (equivalent HRT for the Tatuanui bioreactor calculated from the suggested 6–8 h in a 6.38 m^3 bioreactor) proposed in another study based on minimising the production of both N_2O and CH_4 (Davis et al., 2019). This discrepancy in the preferred HRT could be due to the differences in environmental factors (e.g. temperature, nitrate load, etc.) and bioreactor characteristics (e.g. woodchip material) (Martin et al., 2019), as well as the different gases considered. While both sulphate reduction and CH_4 production provide guidance on the upper limit of HRTs to minimise pollution swapping, our study gave more emphasis on minimising sulphate reduction than on CH_4 production due to the undesirable odour emitted by the former that could negatively influence its adoption by farmers. Moreover, our results also showed that CH_4 production apparently occurred throughout the season and a preferred HRT range, aside from 'the shorter, the better', would be difficult to determine given the limited number of CH_4 measurements made ($n = 9$). Thus, in terms of greenhouse gas production, our study focused more on N_2O given that N_2O is a more potent greenhouse gas (265 times the global warming potential of CO_2) than methane (28 times the potential of CO_2) (Davis et al., 2019). However, nitrate removal efficiency within the above proposed 4–5 days HRT range was lower than desirable (only 40–60%; Fig. 7a and 10). With an average HRT of 4.7 days and a removal efficiency of 48%, the 2018 season fell within this range. This indicates that the release of undesirable dissolved gases from the bioreactor was minimal in the 2018 season, yet the removal efficiency left room for improvement. A HRT range of 5–6 days may be a defensible compromise, as some H_2S production may be tolerable if it ensures high RE and N_2O reduction.

The above observations suggest that manipulating HRT alone will not result in the desired outcome of enhanced nitrate removal with minimal production of undesirable gases. Moreover, given the highly variable nature of flows, an effective HRT manipulation would require a flow control set-up that automatically responds to real-time flows, and this can be costly and not practical or attractive in the actual on-farm application of the bioreactor technology. In addition, flow manipulation would also mean that only a proportion of drainage flow can be treated during high-flow periods. On the other hand, making more carbon available to the microbial community during periods with high nitrate loads (high flow and/or high nitrate concentrations) may help achieve the maximum nitrate removal that is feasible without incurring substantial negative side effects. This may well be accomplished by adding readily available carbon during periods of high flow and/or high nitrate concentrations in the inflow, as we have seen removal efficiency declining with decreasing HRT (Fig. 7a). Limited studies investigating the effect of additional carbon have shown increase in substantial nitrate removal in woodchip bioreactors with the addition of readily available carbon, such as acetate, glucose, methanol, and glycerine (Warneke et al., 2011b; Warneke et al., 2011c; Hartz et al., 2017; Roser et al., 2018). For instance, up to more than double the nitrate RRs were observed when glucose was added to the bioreactor with pine woodchips (Warneke et al., 2011c). Thus, C dosing holds promise to optimise the performance of bioreactors in treating artificial drainage water with variable flow conditions. Limited field-scale studies with C dosing were done mainly to address extremely high nitrate concentrations in the inflow (150–193 mg NO_3-N L^{-1}) (Hartz et al., 2017). Further studies are needed to provide guidance for nitrate concentrations more commonly observed under pastoral agriculture (< 30 mg NO_3-N L^{-1}) and on C dosing operation (the type of C source, frequency, amount, etc.) to minimise potential side effects, including excess DOC in the outflow (Hartz et al., 2017) and clogging by biofilms (Hunter, 2001).

4. Conclusion

The Tatuanui woodchip bioreactor was found to be effective in removing nitrate from subsurface artificial drainage waters at a New Zealand field site with dynamic flow rates and nitrate concentrations. Surprisingly, it also showed its potential to remove DRP from the drainage water at a high rate not yet seen in previous studies. Continued monitoring is needed to confirm the sustainability of this additional desirable property of a woodchip bioreactor. The most obvious factors affecting the nitrate removal capability of the bioreactor include the HRT of the drainage water, availability of electron donor (in this case, organic carbon), and inflow nitrate loads. The first two factors were positively correlated with the removal efficiency, whereas inflow nitrate load was negatively correlated with removal efficiency but positively correlated with removal rate. On the other hand, some negative side effects in the form of pollution swapping were observed. In the initial start-up phase of the bioreactor operation, enhanced release of DOC and DRP was evident. A smaller flush of DOC was also observed at the start of the second drainage season, presumably due to the aerobic conditions in the bioreactor between drainage seasons. Outside this period of annual start-up flush, production of greenhouse (N_2O and CH_4) and odorous gases (H_2S) were observed and influenced by HRT. The undesirable effect of high DOC and DRP concentrations in the early discharges could easily be addressed by applying the first outflow (equivalent to approximately 3 to 3.5 times the bioreactor pore volume) on to the land instead of discharging it to open drains or streams. However, minimising the production of undesirable gases is not as straightforward and cannot solely be addressed by manipulating flow through the bioreactor without compromising nitrate removal. While

longer HRT is needed to minimise dissolved N_2O in the outflow, this could also result in the production of H_2S and CH_4. Therefore, in highly varying drainage flow conditions, the addition of readily available carbon during high flows and/or high nitrate concentrations needs to be considered as feasible procedure to enhance the nitrate removal efficiency of the bioreactor while minimising the production of undesirable gases. Future studies need to focus on the specifics of adding additional readily available carbon to optimise the performance of bioreactors in the treatment of drainage water with highly dynamic inflow characteristics.

Declaration of Competing Interest

None.

Acknowledgements

This work is part of the SSIF-funded 'Enhanced Mitigation of Nitrate in Groundwater' programme led by ESR in collaboration with Lincoln Agritech Ltd., Aqualinc Research Ltd., Southern Geophysical, and University of Canterbury. We gratefully acknowledge the co-funding from the Waikato Regional Council for laboratory analyses in 2017, and the co-operation of the landowners, the Mourits family. We would also like to thank Prof. Louis Schipper (University of Waikato, New Zealand) and Dr. Laura Christianson (University of Illinois at Urbana-Champaign, IL, USA) who shared their knowledge and expertise with us in the planning and design stages, and we are especially grateful to Prof. Schipper who reviewed and provided feedback on a draft of this manuscript. We also thank the four anonymous reviewers for their constructive comments.

References

Addy, K., Gold, A.J., Christianson, L.E., David, M.B., Schipper, L.A., Ratigan, N.A., 2016. Denitrifying Bioreactors for Nitrate Removal: a Meta-Analysis. J. Environ. Qual. 45, 873–881.
Algoazany, A.S., Kalita, P.K., Czapar, G.F., Mitchell, J.K., 2007. Phosphorus transport through subsurface drainage and surface runoff from a flat watershed in east Central Illinois, USA. J. Environ. Qual. 36, 681–693.
Arenas Amado, A., Schilling, K.E., Jones, C.S., Thomas, N., Weber, L.J., 2017. Estimation of tile drainage contribution to streamflow and nutrient loads at the watershed scale based on continuously monitored data. Environ. Monit. Assess. 189, 426.
Ballantine, D.J., Tanner, C.C., 2013. Controlled drainage systems to reduce contaminant losses and optimize productivity from New Zealand pastoral systems. N. Z. J. Agric. Res. 56, 171–185.
Barkle, G.F., Schipper, L.A., Burgess, C.P., Painter, B., 2008. In situ mixing of organic matter decreases hydraulic conductivity of denitrification walls in sand aquifers. Ground Water Monit. Remediat. 28, 57–64.
Blowes, D.W., Robertson, W.D., Ptacek, C., Merkley, C., 1994. Removal of agricultural nitrate from tile-drainage effluent water using in-line bioreactors. J. Contam. Hydrol. 15, 207–221.
Bock, E., Smith, N., Rogers, M., Coleman, B., Reiter, M., Benham, B., Easton, Z.M., 2015. Enhanced nitrate and phosphate removal in a denitrifying bioreactor with biochar. J. Environ. Qual. 44, 605–613.
Bock, E.M., Coleman, B., Easton, Z.M., 2016. Effect of Biochar on Nitrate Removal in a Pilot-Scale Denitrifying Bioreactor. J. Environ. Qual. 45, 762–771.
Bock, E.M., Coleman, B.S.L., Easton, Z.M., 2018a. Effect of biochar, hydraulic residence time, and nutrient loading on greenhouse gas emission in laboratory-scale denitrifying bioreactors. Ecol. Eng. 120, 375–383.
Bock, E.M., Coleman, B.S.L., Easton, Z.M., 2018b. Performance of an under-loaded denitrifying bioreactor with biochar amendment. J. Environ. Manag. 217, 447–455.
Bowman, R.A., Focht, D.D., 1974. The influence of glucose and nitrate concentrations upon denitrification rates in sandy soils. Soil Biology & Biochemistry 6, 297–301.
Bruun, J., Hoffmann, C.C., Kjaergaard, C., 2016a. Nitrogen Removal in Permeable Woodchip Filters Affected by Hydraulic Loading Rate and Woodchip Ratio. J. Environ. Qual. 45, 1688–1695.
Bruun, J., Pugliese, L., Hoffmann, C.C., Kjaergaard, C., 2016b. Solute transport and nitrate removal in full-scale subsurface flow constructed wetlands of various designs treating agricultural drainage water. Ecol. Eng. 97, 88–97.
Bruun, J., Hoffmann, C.C., Kjaergaard, C., 2017. Convective transport of dissolved gases determines the fate of the greenhouse gases produced in reactive drainage filters. Ecol. Eng. 98, 1–10.
Burbery, L., Abraham, P., Afrit, B., 2014. Determining the hydraulic properties of wood/gravel mixtures for use in denitrifying walls. J. Hydrol. (NZ) 53, 1–21.
Cameron, S.G., Schipper, L.A., 2010. Nitrate removal and hydraulic performance of organic carbon for use in denitrification beds. Ecol. Eng. 36, 1588–1595.
Cameron, S.C., Schipper, L.A., 2012. Hydraulic properties, hydraulic efficiency and nitrate removal of organic carbon media for use in denitrification beds. Ecol. Eng. 41, 1–7.
Carstensen, M.V., Larsen, S.E., Kjaergaard, C., Hoffmann, C.C., 2019. Reducing adverse side effects by seasonally lowering nitrate removal in subsurface flow constructed wetlands. J. Environ. Manag. 240, 190–197.
Choudhury, T., Robertson, W.D., Finnigan, D.S., 2016. Suspended Sediment and Phosphorus Removal in a Woodchip Filter System Treating Agricultural Wash Water. J. Environ. Qual. 45, 796–802.
Christianson, L., Castello, A., Christianson, R., Helmers, M., Bhandari, A., 2010. Hydraulic property determination of denitrifying bioreactor fill media. Appl. Eng. Agric. 26, 849–854.
Christianson, L.E., Hanly, J.A., Hedley, M.J., 2011. Optimized denitrification bioreactor treatment through simulated drainage containment. Agric. Water Manag. 99, 85–92.
Christianson, L., Bhandari, A., Helmers, M., 2012a. A practice-oriented review of woodchip bioreactors for subsurface agricultural drainage. Appl. Eng. Agric. 28, 861–874.
Christianson, L., Bhandari, A., Helmers, M., Kult, K., Sutphin, T., Wolf, R., 2012b. Performance evaluation of four field-scale agricultural drainage denitrification bioreactors in Iowa. Trans. ASABE 55, 2163–2174.
Christianson, L., Hanly, J., Jha, N., Saggar, S., Hedley, M., 2013a. Denitrification bioreactor nitrous oxide emissions under fluctuating conditions. In: ASABE Meeting Paper, Paper no. 131597821. 7.
Christianson, L., Helmers, M., Bhandari, A., Moorman, T., 2013b. Internal hydraulics of an agricultural drainage denitrification bioreactor. Ecol. Eng. 52, 298–307.
Christianson, L.E., Collick, A.S., Bryant, R.B., Rosen, T., Bock, E.M., Allen, A.L., Kleinman, P.J.A., May, E.B., Buda, A.R., Robinson, J., Folmar, G.J., Easton, Z.M., 2017a. Enhanced denitrification bioreactors hold promise for mid-atlantic ditch drainage. Agricult. Environ. Lett. 2, 1–5.
Christianson, L.E., Lepine, C., Sibrell, P.L., Penn, C., Summerfelt, S.T., 2017b. Denitrifying woodchip bioreactor and phosphorus filter pairing to minimize pollution swapping. Water Res. 121, 129–139.
Christianson, L.E., Feyereisen, G., Lepine, C., Summerfelt, S.T., 2018. Plastic carrier polishing chamber reduces pollution swapping from denitrifying woodchip bioreactors. Aquac. Eng. 81, 33–37.
Chun, J.A., Cooke, R.A., Eheart, J.W., Cho, J., 2010. Estimation of flow and transport parameters for woodchip-based bioreactors: II. Field-scale bioreactor. Biosyst. Eng. 105, 95–102.
David, M.B., Gentry, L.E., Cooke, R.A., Herbstritt, S.M., 2016. Temperature and substrate control woodchip bioreactor performance in reducing Tile nitrate loads in East-Central Illinois. J. Environ. Qual. 45, 822–829.
Davis, M.P., Martin, E.A., Moorman, T.B., Isenhart, T.M., Soupir, M.L., 2019. Nitrous oxide and methane production from denitrifying woodchip bioreactors at three hydraulic residence times. J. Environ. Manag. 242, 290–297.
Eckard, R.J., White, R.E., Edis, R., Smith, A., Chapman, D.F., 2004. Nitrate leaching from temperate perennial pastures grazed by dairy cows in South-Eastern Australia. Aust. J. Agric. Res. 55, 911.
Elgood, Z., Robertson, W.D., Schiff, S.L., Elgood, R., 2010. Nitrate removal and greenhouse gas production in a stream-bed denitrifying bioreactor. Ecol. Eng. 36, 1575–1580.
Fenton, O., Healy, M.G., Brennan, F.P., Thornton, S.F., Lanigan, G.J., Ibrahim, T.G., 2016. Holistic evaluation of field-scale denitrifying bioreactors as a basis to improve environmental sustainability. J. Environ. Qual. 45, 788–795.
Feyereisen, G.W., Christianson, L., 2015. Hydraulic flow characteristics of agricultural residues for denitrifying bioreactor media. Appl. Eng. Agric. 31, 89–96.
Ghane, E., Fausey, N.R., Brown, L.C., 2015. Modeling nitrate removal in a denitrification bed. Water Res. 71, 294–305.
Ghane, E., Feyereisen, G.W., Rosen, C.J., 2016. Non-linear hydraulic properties of woodchips necessary to design denitrification beds. J. Hydrol. 542, 463–473.
Ghane, E., Feyereisen, G.W., Rosen, C.J., 2019. Efficacy of bromide tracers for evaluating the hydraulics of denitrification beds treating agricultural drainage water. J. Hydrol. 574, 129–137.
Goeller, B.C., Burbery, L.F., Febria, C.M., Collins, K.E., Burrows, N.J., Simon, K.S., Harding, J.S., McIntosh, A.R., 2019. Capacity for bioreactors and riparian rehabilitation to enhance nitrate attenuation in agricultural streams. Ecol. Eng. 134, 65–77.
Goodwin, G.E., Bhattarai, R., Cooke, R., 2015. Synergism in nitrate and orthophosphate removal in subsurface bioreactors. Ecol. Eng. 84, 559–568.
Gottschall, N., Edwards, M., Craiovan, E., Frey, S.K., Sunohara, M., Ball, B., Zoski, E., Topp, E., Khan, I., Clark, I.D., Lapen, D.R., 2016. Amending woodchip bioreactors with water treatment plant residuals to treat nitrogen, phosphorus, and veterinary antibiotic compounds in tile drainage. Ecol. Eng. 95, 852–864.
Greenan, C.M., Moorman, T.B., Parkin, T.B., Kaspar, T.C., Jaynes, D.B., 2009. Denitrification in wood chip bioreactors at different water flows. J. Environ. Qual. 38, 1664–1671.
Griessmeier, V., Leberecht, K., Gescher, J., 2019. NO3 (−) removal efficiency in field denitrification beds: key controlling factors and main implications. Environ. Microbiol. Rep. 11, 316–329.
Hartz, T., Smith, R., Cahn, M., Bottoms, T., Bustamante, S.C., Tourte, L., Johnson, K., Coletti, L., 2017. Wood chip denitrification bioreactors can reduce nitrate in tile drainage. Calif. Agric. 71, 41–47.
Hassanpour, B., Giri, S., Pluer, W.T., Steenhuis, T.S., Geohring, L.D., 2017. Seasonal performance of denitrifying bioreactors in the Northeastern United States: field trials. J. Environ. Manag. 202, 242–253.
Healy, M.G., Ibrahim, T.G., Lanigan, G.J., Serrenho, A.J., Fenton, O., 2012. Nitrate removal rate, efficiency and pollution swapping potential of different organic carbon

media in laboratory denitrification bioreactors. Ecol. Eng. 40, 198–209.
Healy, M.G., Barrett, M., Lanigan, G.J., João Serrenho, A., Ibrahim, T.G., Thornton, S.F., Rolfe, S.A., Huang, W.E., Fenton, O., 2015. Optimizing nitrate removal and evaluating pollution swapping trade-offs from laboratory denitrification bioreactors. Ecol. Eng. 74, 290–301.
Herbstritt, S.M., 2014. Environmental tradeoffs of denitrifying woodchip bioreactors. Vol. M Sc. University of Illinois at Urbana-Champaign, pp. 93.
Hoover, N.L., Bhandari, A., Soupir, M.L., Moorman, T.B., 2016. Woodchip denitrification bioreactors: impact of temperature and hydraulic retention time on nitrate removal. J. Environ. Qual. 45, 803–812.
Hua, G., Salo, M.W., Schmit, C.G., Hay, C.H., 2016. Nitrate and phosphate removal from agricultural subsurface drainage using laboratory woodchip bioreactors and recycled steel byproduct filters. Water Res. 102, 180–189.
Hudson, N., McKergow, L., Tanner, C.C., Baddock, E., Burger, D., Scandrett, J., 2018. Denitrification bioreactor work in Waituna Lagoon Catchment, Southland. In: Currie, L., Christensen, C. (Eds.), Farm Environmental Planning - Science, Policy, and Practice. 31. Fertilizer and Lime Research Centre, Massey University, Palmerston North, New Zealand, pp. 1–10.
Hunter, W., 2001. Use of vegetable oil in a pilot-scale denitrifying barrier. J. Contam. Hydrol. 53, 119–131.
Husk, B.R., Anderson, B.C., Whalen, J.K., Sanchez, J.S., 2017. Reducing nitrogen contamination from agricultural subsurface drainage with denitrification bioreactors and controlled drainage. Biosyst. Eng. 153, 52–62.
Husk, B.R., Sanchez, J.S., Anderson, B.C., Whalen, J.K., Wootton, B.C., 2018. Removal of phosphorus from agricultural subsurface drainage water with woodchip and mixed-media bioreactors. J. Soil Water Conserv. 73, 265–275.
Jaynes, D.B., Kaspar, T.C., Moorman, T.B., Parkin, T.B., 2008. In situ bioreactors and deep drain-pipe installation to reduce nitrate losses in artificially drained fields. J. Environ. Qual. 37, 429–436.
Johansson Westholm, L., 2006. Substrates for phosphorus removal-potential benefits for on-site wastewater treatment? Water Res. 40, 23–36.
Jurado, A., Borges, A.V., Brouyere, S., 2017. Dynamics and emissions of N2O in groundwater: a review. Sci. Total Environ. 584–585, 207–218.
King, K.W., Williams, M.R., Fausey, N.R., 2015a. Contributions of systematic tile drainage to watershed-scale phosphorus transport. J. Environ. Qual. 44, 486–494.
King, K.W., Williams, M.R., Macrae, M.L., Fausey, N.R., Frankenberger, J., Smith, D.R., Kleinman, P.J., Brown, L.C., 2015b. Phosphorus transport in agricultural subsurface drainage: a review. J. Environ. Qual. 44, 467–485.
Lepine, C., Christianson, L., Sharrer, K., Summerfelt, S., 2016. Optimizing hydraulic retention times in denitrifying woodchip bioreactors treating recirculating aquaculture system wastewater. J. Environ. Qual. 45, 813–821.
Long, L.M., Schipper, L.A., Bruesewitz, D.A., 2011. Long-term nitrate removal in a denitrification wall. Agric. Ecosyst. Environ. 140, 514–520.
Martin, E.A., Davis, M.P., Moorman, T.B., Isenhart, T.M., Soupir, M.L., 2019. Impact of hydraulic residence time on nitrate removal in pilot-scale woodchip bioreactors. J. Environ. Manag. 237, 424–432.
Maxwell, B.M., Birgand, F., Schipper, L.A., Christianson, L.E., Tian, S., Helmers, M.J., Williams, D.J., Chescheir, G.M., Youssef, M.A., 2019. Drying-rewetting cycles affect nitrate removal rates in woodchip bioreactors. J. Environ. Qual. 48, 93–101.
McMahon, P.B., Chapelle, F.H., 2008. Redox processes and water quality of selected principal aquifer systems. Ground Water 46, 259–271.
McWilliam, I.G., Dewar, R.A., 1958. Flame ionization detector for gas chromatography. Nature 181, 760.
Mosier, A.R., Mack, L., 1980. Gas Chromatographic System for Precise, Rapid Analysis of Nitrous Oxide. Soil Sci. Soc. Am. J. 44, 1121–1123.
Nordström, A., Herbert, R.B., 2019. Identification of the temporal control on nitrate removal rate variability in a denitrifying woodchip bioreactor. Ecol. Eng. 127, 88–95.
Pfannerstill, M., Kühling, I., Hugenschmidt, C., Trepel, M., Fohrer, N., 2016. Reactive ditches: a simple approach to implement denitrifying wood chip bioreactors to reduce nitrate exports into aquatic ecosystems? Environ. Earth Sci. 75.
Rambags, F., Tanner, C.C., Stott, R., Schipper, L.A., 2016. Fecal bacteria, bacteriophage, and nutrient reductions in a full-scale denitrifying woodchip bioreactor. J. Environ. Qual. 45, 847–854.
Rice, E.W., Baird, R.B., Eaton, A.D., Clesceri, L.S., 2012. Standard Methods for the Examination of Water and Wastewater. American Public Health Association, American Water Works Association, Water Environment Federation (1496 pp).
Rivas, A., Singh, R., Horne, D., Roygard, J., Matthews, A., Hedley, M.J., 2017. Denitrification potential in the subsurface environment in the Manawatu River catchment, New Zealand: Indications from oxidation-reduction conditions, hydrogeological factors, and implications for nutrient management. J. Environ. Manag. 197, 476–489.
Rivett, M.O., Buss, S.R., Morgan, P., Smith, J.W., Bemment, C.D., 2008. Nitrate attenuation in groundwater: a review of biogeochemical controlling processes. Water Res. 42, 4215–4232.
Robertson, W.D., Merkley, L.C., 2009. In-stream bioreactor for agricultural nitrate treatment. J. Environ. Qual. 38, 230–237.
Robertson, W.D., Blowes, D.W., Ptacek, C., Cherry, J.A., 2000. Long-term performance of in situ reactive barriers for nitrate remediation. Ground Water 38, 689–695.
Robertson, W.D., Ptacek, C., Brown, S., 2009. Rates of nitrate perchlorate removal in a 5-year-old wood particle reactor treating agricultural drainage. Ground Water Monit. Remediat. 29, 87–94.
Robertson, W.D., Feng, D., Kobylinski, S., Finnigan, D.S., Merkley, C., Schiff, S.L., 2018. Low cost media can filter particulate phosphorus from turbid stream water under short retention times. Ecol. Eng. 123, 95–102.
Roser, M.B., Feyereisen, G.W., Spokas, K.A., Mulla, D.J., Strock, J.S., Gutknecht, J., 2018. Carbon dosing increases nitrate removal rates in denitrifying bioreactors at low-temperature high-flow conditions. J. Environ. Qual. 47, 856–864.
Sarris, T.S., Burbery, L.F., 2018. Stochastic multi-objective performance optimization of an in-stream woodchip denitrifying bioreactor. Ecol. Eng. 124, 38–50.
Schipper, L.A., Vojvodic-Vukovic, M., 1998. Nitrate removal from groundwater using a denitrification wall amended with sawdust: field trial. J. Environ. Qual. 27, 664–668.
Schipper, L.A., Barkle, G.F., Hadfield, J.C., Vojvodic-Vukovic, M., Burgess, C.P., 2004. Hydraulic constraints on the performance of a groundwater denitrification wall for nitrate removal from shallow groundwater. J. Contam. Hydrol. 69, 263–279.
Schipper, L.A., Barkle, G.F., Vojvodic-Vukovic, M., 2005. Maximum rates of nitrate removal in a denitrification wall. J. Environ. Qual. 34, 1270–1276.
Schipper, L.A., Robertson, W.D., Gold, A.J., Jaynes, D.B., Cameron, S.C., 2010. Denitrifying bioreactors—an approach for reducing nitrate loads to receiving waters. Ecol. Eng. 36, 1532–1543.
Sharrer, K.L., Christianson, L.E., Lepine, C., Summerfelt, S.T., 2016. Modeling and mitigation of denitrification 'woodchip' bioreactor phosphorus releases during treatment of aquaculture wastewater. Ecol. Eng. 93, 135–143.
Soupir, M.L., Hoover, N.L., Moorman, T.B., Law, J.Y., Bearson, B.L., 2018. Impact of temperature and hydraulic retention time on pathogen and nutrient removal in woodchip bioreactors. Ecol. Eng. 112, 153–157.
Spalding, R., Parrot, J., 1994. Shallow groundwater denitrification. Sci. Total Environ. 141, 17–25.
Stenger, R., Clague, J.C., Morgenstern, U., Clough, T.J., 2018. Vertical stratification of redox conditions, denitrification and recharge in shallow groundwater on a volcanic hillslope containing relict organic matter. Sci. Total Environ. 639, 1205–1219.
Tan, C.S., Drury, C.F., Gaynor, J.D., Ng, H.Y.F., 1999. Effect of controlled drainage and subirrigation on subsurface Tile drainage nitrate loss and crop yield at the farm scale. Can. Water Resour. J. 24, 177–186.
Tanner, C.C., Long Nguyen, M., Sukias, J.P.S., 2003. Using constructed wetlands to treat subsurface drainage from intensively grazed dairy pastures in New Zealand. Water Sci. Technol. 48, 207–213.
Tanner, C.C., Sukias, J.P.S., Headley, T.R., Yates, C.R., Stott, R., 2012. Constructed wetlands and denitrifying bioreactors for on-site and decentralised wastewater treatment: Comparison of five alternative configurations. Ecol. Eng. 42, 112–123.
Tchobanoglous, G., David Stensel, H., Tsuchihashi, R., Burton, F.L., 2014. Wastewater engineering: treatment and resource recovery, Fifth edition. New York, McGRaw-Hill Education, New York 2018 pages.
van Driel, P.W., Robertson, W.D., Merkley, L.C., 2006. Denitrification of agricultural drainage using wood-based reactors. Trans. ASABE 49, 565–573.
Vohla, C., Kõiv, M., Bavor, H.J., Chazarenc, F., Mander, Ü., 2011. Filter materials for phosphorus removal from wastewater in treatment wetlands—a review. Ecol. Eng. 37, 70–89.
von Ahnen, M., Pedersen, P.B., Dalsgaard, J., 2016. Start-up performance of a woodchip bioreactor operated end-of-pipe at a commercial fish farm—a case study. Aquac. Eng. 74, 96–104.
Warneke, S., Schipper, L.A., Bruesewitz, D.A., Baisden, W.T., 2011a. A comparison of different approaches for measuring denitrification rates in a nitrate removing bioreactor. Water Res. 45, 4141–4151.
Warneke, S., Schipper, L.A., Bruesewitz, D.A., McDonald, I., Cameron, S., 2011b. Rates, controls and potential adverse effects of nitrate removal in a denitrification bed. Ecol. Eng. 37, 511–522.
Warneke, S., Schipper, L.A., Matiasek, M.G., Scow, K.M., Cameron, S., Bruesewitz, D.A., McDonald, I.R., 2011c. Nitrate removal, communities of denitrifiers and adverse effects in different carbon substrates for use in denitrification beds. Water Res. 45, 5463–5475.
Weigelhofer, G., Hein, T., 2015. Efficiency and detrimental side effects of denitrifying bioreactors for nitrate reduction in drainage water. Environ. Sci. Pollut. Res. 22, 13534–13545.
Zoski, E., Lapen, D.R., Gottschall, N., Murrell, R., Schuba, B., 2013. Nitrogen, phosphorus, and bacterial removal in laboratory-scale woodchip bioreactors amended with drinking water treatment residuals. Trans. ASABE 56, 1339–1347.